Prepared for the
Florida Department of Transportation
FDOT Contract Number BDK75 977-15

Use of Scanning Electron Microscopy and Microanalysis to Determine Chloride Content of Concrete and Raw Materials

Final Report Draft

July 25, 2013

DISCLAIMER

"The opinions, findings, and conclusions expressed in this publication are those of the authors and not necessarily those of the State of Florida Department of Transportation."

METRIC CONVERSION TABLE

APPROXIMATE CONVERSIONS TO SI UNITS

SYMBOL	WHEN YOU KNOW	MULTIPLY BY	TO FIND	SYMBOL
		LENGTH		
in	inches	25.4	millimeters	mm
ft	feet	0.305	meters	m
yd	yards	0.914	meters	m
mi	miles	1.61	kilometers	km
		AREA		
in^2	squareinches	645.2	square millimeters	mm^2
ft^2	squarefeet	0.093	square meters	m^2
yd^2	square yard	0.836	square meters	m^2
ac	acres	0.405	hectares	ha
mi^2	square miles	2.59	square kilometers	km^2
		VOLUME		
fl oz	fluid ounces	29.57	milliliters	mL
gal	gallons	3.785	liters	L
ft^3	cubic feet	0.028	cubic meters	m^3
yd^3	cubic yards	0.765	cubic meters	m^3
		MASS		
oz	ounces	28.35	grams	g
lb	pounds	0.454	kilograms	kg
T	short tons (2000 lb)	0.907	megagrams (or "metric ton")	Mg (or "t")
		TEMPERATURE (exact degrees)		
^oF	Fahrenheit	5 (F-32)/9 or (F-32)/1.8	Celsius	^oC

APPROXIMATE CONVERSIONS TO SI UNITS

SYMBOL	WHEN YOU KNOW	MULTIPLY BY	TO FIND	SYMBOL
		LENGTH		
mm	millimeters	0.039	inches	in
m	meters	3.28	feet	ft
m	meters	1.09	yards	yd
km	kilometers	0.621	miles	mi
		AREA		
mm^2	square millimeters	0.0016	square inches	in^2
m^2	square meters	10.764	square feet	ft^2
m^2	square meters	1.195	square yards	yd^2
ha	hectares	2.47	acres	ac
km^2	square kilometers	0.386	square miles	mi^2
		VOLUME		
mL	milliliters	0.034	fluid ounces	fl oz
L	liters	0.264	gallons	gal
m^3	cubic meters	35.314	cubic feet	ft^3
m^3	cubic meters	1.307	cubic yards	yd^3
		MASS		
g	grams	0.035	ounces	oz
kg	kilograms	2.202	pounds	lb
Mg (or "t")	megagrams (or "metric ton")	1.103	short tons (2000 lb)	T
		TEMPERATURE (exact degrees)		
^oC	Celsius	1.8C+32	Fahrenheit	^oF

TECHNICAL REPORT DOCUMENTATION

1. Report No.	2. Government Accession No.	3. Recipient's Catalog No.
4. Title and Subtitle Use of Scanning Electron Microscopy and Microanalysis to Determine Chloride Content of Concrete and Raw Materials		5. Report Date February 14, 2013
		6. Performing Organization Code
7. Author(s) Luisa Amelia Dempere, Bradley Willenberg, Richard Deist		8. Performing Organization Report No.
9. Performing Organization Name and Address Major Analytical Instrumentation Center (MAIC), College of Engineering, University of Florida, P.O. Box 116400, Gainesville, Florida, 32611		10. Work Unit No. (TRAIS)
		11. Contract or Grant No. BDK75 977-15
12. Sponsoring Agency Name and Address Florida Department of Transportation 605 Suwannee Street, MS 30 Tallahassee, FL 32399		13. Type of Report and Period Covered
		14. Sponsoring Agency Code
15. Supplementary Notes		

16. Abstract

Standard sample sets of cement and mortar formulations with known levels of Cl as well as concrete samples subject to Cl diffusion were all prepared for and analyzed with scanning electron microscopy (SEM) and electron microprobe (EPMA). Using x-ray spectroscopic data generated with these instruments large scale (cm^2) elemental distribution maps were constructed for the standard samples sets and used to calibrate each instrument for future quantitative analysis of cementitious samples. Quantitative distribution maps using both the SEM and EPMA instruments were constructed for all concrete samples subject to Cl diffusion. Cl diffusion profiles comparing wet chemistry and microanalysis were generated from the quantitative map images of all samples. Mathematical fitting of normalized diffusion profiles generated with data from both instruments was used to determine Cl diffusivity (D_a) in all samples subject to diffusion and was compared to the D_a determined by wet chemistry. Analysis time for the largest areas studied took ≈8hr using the SEM and ≈30hr using the EPMA. Comparison of the Cl concentration data from both SEM and EPMA indicates that both methods consistently over-predict the Cl concentration at a given depth compared to wet chemistry. The over-prediction indicates that the standard sets used are not the most appropriate for these methods. This contention is well supported by the fact that using one of the diffusion-subject samples as a calibration standard yielded absolute concentrations for the other diffusion-subject similar to those determined by wet chemistry. Normalization and comparison of all data from wet chemistry and both instruments obviated the need for standards and generated D_a's for all diffusion-subject samples within 6.8% and 4.4% error for EDS and WDS respectively compared to wet chemistry. These x-ray microanalysis methods therefore not only yield new data detailing the microscopic spatial distribution of Cl in cementitious materials, but could also be used in a streamlined approach to determine D_a of Cl more rapidly than the wet chemical analysis techniques currently employed.

17. Key Word	18. Distribution Statement
Cl diffusion, concrete, cement, SEM, EPMA, concentration profiles, microanalysis, EDS	No restrictions.

19. Security Classif. (of this report)	20. Security Classif. (of this page)	21. No. of Pages	22. Price
Unclassified.	Unclassified.		

ACKOWLEDGEMENTS

The authors (Luisa A. Dempere, Brad Willenberg, and Richard Deist) would like to thank the financial support of the Florida Department of Transportation's State Materials Office for the work presented in this report. We would also want to express our gratitude to Mario Paredes and Ron Simmons for all the help with the supply of samples, fruitful discussions, constant stimulus and support. Our thanks to Sandra Bell for keeping us on track with our deadlines, and Wayne Acree for providing advice, help and expertise to the project.

PREFACE

In the fall of 2009 the Florida Department of Transportation's State Materials Office (FDOT-SMO) in Gainesville, Florida, approved a grant to develop an appropriate method of "Use of Scanning Electron Microscopy and Microanalysis to Determine Chloride Content of Concrete and Raw Materials". The method was to be developed at the Major Analytical Instrumentation Center (MAIC), one of the research service centers within the University of Florida's College of Engineering under contract BDK75 977-15. FDOT-SMO would provide standard cementitious samples and evaluate the potential of the method to augment and/or replace the analytical techniques currently practiced by FDOT-SMO for analysis of chloride in cementitious materials. An electron microscope-based method has significant advantages and the motivations for the contract were clear: 1) automated and non-destructive sample analysis, 2) generation of never-before seen quantitative microscopic images of the chloride distribution over large areas (cm^2) of sample materials and 3) minimization of both the use of harsh chemicals and generation of hazardous wastes. It was further hoped that this electron microscope-based method could more rapidly determine the diffusivity of chloride ions through cementitious samples, thereby increasing sample throughput and helping FDOT-SMO meet its goals and mission. With these common goals, analytical project work began in 2009.

EXECUTIVE SUMMARY

Chloride (Cl) content was analyzed using x-ray analysis techniques (XRT) in cement, mortar and concrete samples subjected to Cl diffusion, and the results were compared with analysis done using wet chemistry (WC). The two XRT used were Scanning Electron Microscopy (SEM) – Energy Dispersive Spectroscopy (EDS), and Electron Probe Microanalysis (EPMA) – Wavelength Dispersive Spectroscopy (WDS). Cement and mortar samples with known levels of Cl were measured and used as a reference for the XRT quantitative measurements. The XRT allowed the construction of quantitative distribution maps of Cl for the concrete samples. From the quantitative Cl distribution maps diffusion profiles were created comparing WC and XRT data. Finally, diffusion profiles were generated and Cl diffusivity (D_a) was evaluated in all the concrete samples. The obtained diffusivity values were compared to the values determined by WC.

The analysis of the samples in this study took approximately 8 hours using the SEM-EDS and 30 hours using the EPMA-WDS. The size of the areas analyzed in the samples was the largest we were able to accommodate with the instruments used. It is expected that the analysis of smaller areas could improve analysis time without significant loss of accuracy. Both SEM-EDS and EPMA-WDS consistently over-predicted the Cl concentration at a given depth in the samples as compared to WC. This result indicated that better reference samples are needed to be used for XRT. When one of the concrete samples was used as a reference, absolute concentrations measured with the x-ray analysis techniques were more similar to those determined by WC. The evaluation of a standardless determination of D_a values was also conducted and applied to all of the concrete samples. This resulted in D_a values that differed from WC results by a maximum of 6.8% and 4.4% for SEM-EDS and EPMA-WDS, respectively. Thus, these XRT have the potential to become a streamlined approach for rapidly determining D_a values at the same time bringing the advantage of providing detailed data on the spatial distribution of Cl in the sample.

TABLE OF CONTENTS

LIST OF ABBREVIATIONS AND TERMS

σ	standard deviation
APS	American Petrographic Service
AU	arbitrary units
BSE	backscattered electrons
CRT	cathode ray tube
EDS	energy dispersive spectroscopy
EH&S	environmental health and safety
EPMA	electron probe micro-analysis
FDOT	Florida Department of Transportation
LOD	limit of detection
MAIC	Major Analytical Instrumentation Center
NaN	not a numeric value
N_b	count rate measured of the background
N_p	count rate observed for the peak and
SE	secondary electrons
SEM	scanning electron microscopy
SC	specimen current
SMO	State Materials Office
ROI	region of interest
TSV	tab-separated variable
UF	University of Florida
V	variance
w/c	water cement ratio
WC	wet chemistry
WDS	wavelength dispersive spectroscopy
XRT	x-ray analysis techniques

LIST OF FIGURES

LIST OF TABLES

CHAPTER 1
INTRODUCTION

Background

Cement and cement-based materials like mortar and concrete are among the most commonly used construction materials worldwide. Known to the ancients, cement, the essential binder in cementitious materials, is composed mainly of anhydrous minerals called calcium silicates that, when mixed with water, react and are converted into various calcium silicate-hydrate crystalline minerals. During curing/setting, all of the various hydration reactions of the minerals form and grow crystals that are entangled and intertwined with the other crystals to ultimately produce a rigid material. Because the various hydration reactions of the several anhydrous minerals are rarely complete at the time the material is considered rigid and cured, cement based materials may continue to harden over the course of many years. Hence in a very real sense, cementitious materials are a sort of dynamic material.

Objects and structures are rarely made solely of cement due to cost and materials properties, thus composites are therefore common. Mortar (cement combined with sand) and concrete (cement combined with sand- fine aggregate rock- large aggregate and other additives like fly-ash, slag, etc.) are the most common and important. Concrete is used frequently as a major structural element in the construction of bridges, roads and buildings. Typically and depending of the specific formulations, concrete has excellent compressive mechanical properties, but is poor in tension, torsion and bending. Concrete is therefore reinforced with steel bars (rebars) to circumvent these limitations in mechanical properties.

Due to the porous nature, structure and composition of cement and concrete, they are permeable to water and ions. This characteristic of concrete can have important consequences on the life time or durability of reinforced concrete structures. It is especially important for structures like bridges and roads in water environments with significant concentrations of chloride. Over time, chloride ions are known to diffuse through the pores and paste component in sufficient quantities to depassivate the surface of the steel rebar and initiate/facilitate rebar corrosion. The main difficulty associated with this type of corrosion is not the loss of strength of the rebar as one might initially suspect, but rather the effective increase in the rebar volume due to the rusting of its surface. The rusty iron phase has a larger volume than its parent iron phase; the rebar begins to swell and exert a pressure/force inside its rigid concrete container. If oxidative conditions persist and the rebar corrosion goes unchecked, the concrete will eventually cracks and spall, potentially further exposing the rebar to corrosive environments.

The Florida Department of Transportation (FDOT) has a deep interest in monitoring chloride ions diffusion in cement and concrete structures as it has many at-risk structures under its upkeep given the unique Florida environment. Ideally FDOT would like to get 75 years out of a structure before major repair, remediation or outright replacement. As chloride-based attack corrosion is a central issue impacting structure durability for FDOT, an in-house chloride monitoring system has been developed and put in place and maintained by the FDOT through their state materials office (SMO) located in Gainesville, Florida. Samples that have been cored from structures like bridge piles and foundations in chloride-rich aqueous environments are routinely analyzed and profiled by FDOT-SMO to assess structure durability and develop chloride-remediation, and repair plans and strategies.

The basic analysis starts by sectioning one of the cored samples at regular thicknesses (often ¼” = 6.35 mm.) starting the exposed surface to the rebar-concrete interface. The sections are then pulverized and digested using nitric acid and the resulting solution titrated with a standardized silver nitrate solution to determine the total chloride content. The titration endpoint is determined potentiometrically via a silver/chloride selective electrode. Although this method is extremely accurate and sensitive for the measurement of total chloride ion content in the slices, it is time consuming and arduous, destroys the sample, yields only one data point per slice, has poor spatial resolution and provides no information about the in situ spatial distribution of chloride ions in the sample.

Statement of Hypothesis

A non-destructive, high spatial resolution method of Cl analysis that provides spatial distribution of Cl in the sample, concentration profiles and diffusion coefficients can be developed using electron beam instrumentation and corresponding x-ray spectroscopy techniques.

Objectives

1. Characterize the microstructure, and Cl elemental composition in the cement paste and concrete samples.
2. Develop a reliable and reproducible method to determine, quantitatively, the chloride ion concentration in cement paste, and concrete samples with known chloride ion concentrations using x-ray microanalysis techniques.

CHAPTER 2
LITERATURE REVIEW

Review of previous research

Two previous studies are key background for the microprobe portion of the microanalysis in this study: “Chloride Ingress Profiles Measured by Electron Probe Micro Analysis” by Jensen *et al.* [5], and “Application for Electron Probe Microanalyzer for Measurement of Cl Concentration Profile in Concrete” by Mori *et al.* [6].

In the Jensen study [5], the e-beam was scanned (stage scanned we assume) in lines (linescans) on a concrete sample surface from the chloride-exposed edge to a depth of 25 mm. normal to the exposed surface. Chloride concentrations were reported as counts of Cl x-rays. The lines consisted of 250 - 1000 points per line with a dwell time of one second per point operating in what the authors called “qualitative measurements” mode. The linescans presented for samples subjected to Cl ingress with water/cement (w/c) ratios = 0.3 showed a decreasing profile in counts as a function of depth from the exposed surface. The data in this study is still raw, but demonstrates that electron probe microanalysis (EPMA) can be used to generate a Cl profile in concrete samples. The authors also determined that epoxy used to fill pores and cracks in the sample can have a detectable level of Cl. Use of standard epoxies in sample preparation should therefore be avoided if possible.

Mori *et al.* [5] conducted a more extensive study and used the EPMA to generate large scale (cm^2) quantitative x-ray maps. These authors used a stage rastering method to collect large-pixel-array ($>10^5$ pixels) x-ray-map images of cement and concrete samples. By using an extremely short dwell time of 40 ms/pixel, large maps could be collected in manageable time frames. These authors also determined that using a defocused probe (50um in diameter), 100 nA probe current, 15 KeV accelerating voltage, a pixel size (step size) of 100 µm yielded a high-quality quantifiable elemental distribution (x-ray map). Cement standards with known levels of Cl (0, 0.5, 1.0, 2.0, 3.0, 4.0, 5.0 wt. %) were also mapped and used to construct linear calibration curves of counts (normalized to probe current) as a function of Cl concentration.

The instrument used in this study was an EPMA equipped with four spectrometers to collect the elements (singly): Cl, Ca, Si, and S. A gating strategy based on the Ca/Si/S ratio determined for each pixel was used to determine which pixels corresponded to aggregate or paste. This strategy allowed for the discrimination between paste and aggregate. A main thrust in the Mori et al. work is that Cl ions diffuse mainly through the paste component of concrete and mortar and minimally through the aggregate components. Quantifying only the Cl in the paste pixels produced Cl concentration/diffusion profiles that essentially matched those obtained through the sectioning/grinding and wet chemistry method used in Japan. Calculated average diffusion coefficients (D_a) obtained from the Cl paste-only maps of 0.5 w/c concrete samples were the same as those obtained for the wet-chemical analysis of similar samples. This correspondence was also maintained for 0.4 w/c samples, however the data point reported for the 0.3 w/c sample was significantly higher than that determined from the wet chemistry data. In light of these results, the x-ray mapping method appeared to be highly effective using the indicated instruments by these authors.

<u>Summary of state-of-the-art</u>

The scanning electron microscope (SEM) used for microanalysis is equipped with an energy dispersive spectroscopy (EDS) system and an electron probe micro-analysis instrument (EPMA) equipped with a wavelength dispersive x-ray spectroscopy (WDS) system was also used. In these instruments, a beam of electrons (e-beam) is generated at the top of a column (electron gun) by a source (filament) (Figure 1) [1], a high potential anode just below the source is strongly positively biased accelerates source electrons down the microscope column. A series of electron lenses in the column “steer” these accelerated electrons down the column and ultimately onto a very fine point on a sample placed on a stage inside of a large chamber. The entire system (gun, column and sample chamber) is maintained under high vacuum conditions essentially to maximize the mean free path of the beam electrons and the electron signal coming out of the sample (Figure 2) [1].

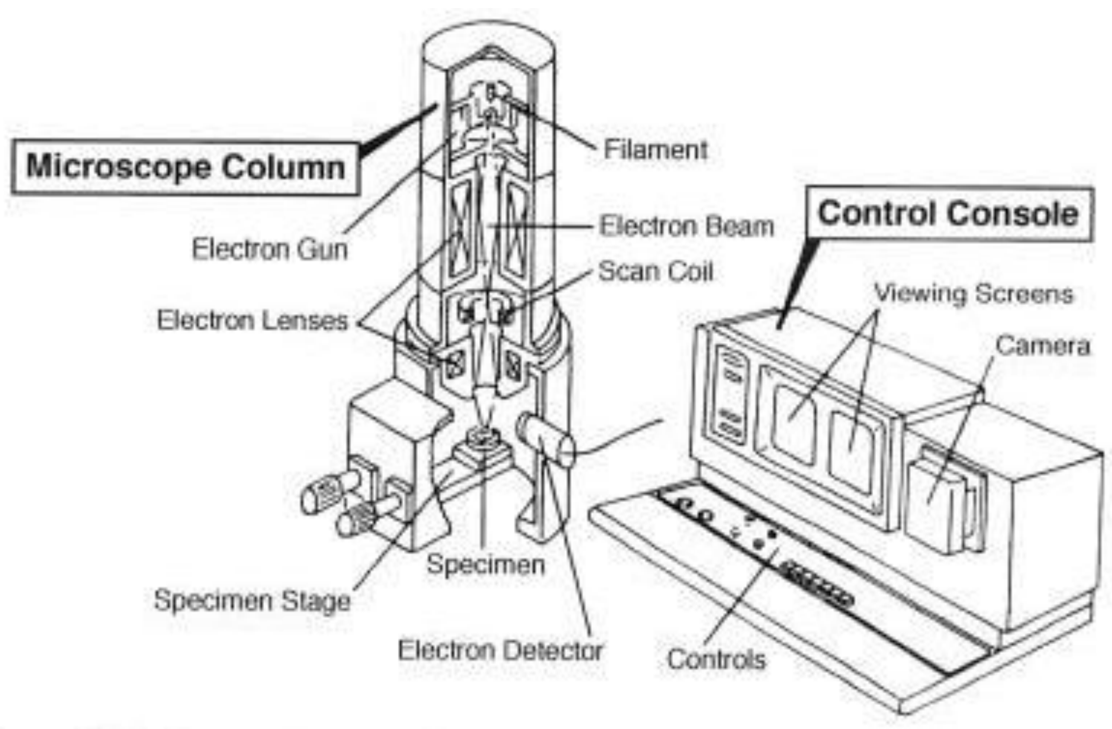

Figure 1 Major parts and components of the SEM [1]

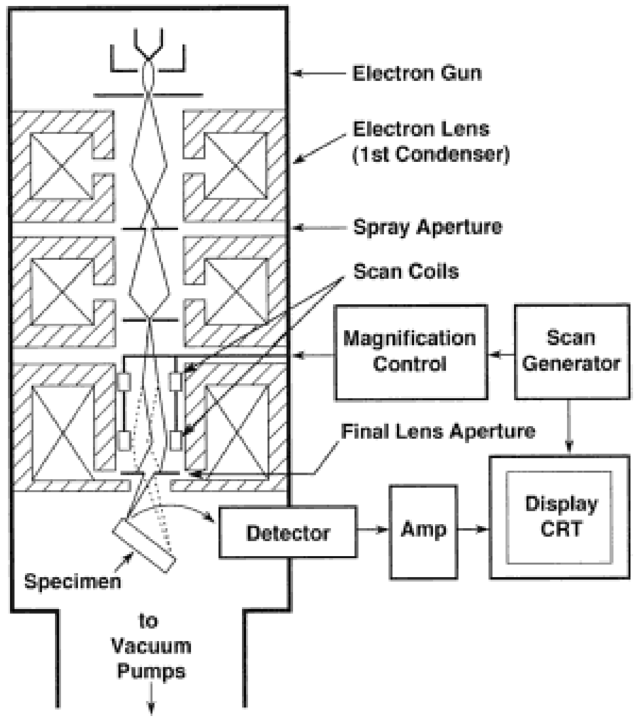

Figure 2 Schematic drawing of the microscope column showing the electron gun, lenses, deflection system, and electron detector [1]

Several physical phenomena occur as the electrons of the beam interact with the atoms of the sample, and multiple signals are generated. These different signals can be broadly categorized into two types: electrons and "light". In the electron category, secondary electrons (SE) are a type of signal composed of low-energy, trajectory independent electrons produced by the sample subsequent to e-beam impingement which provide topographic information about the sample surface that allow for construction of microscopic images of the sample surface.

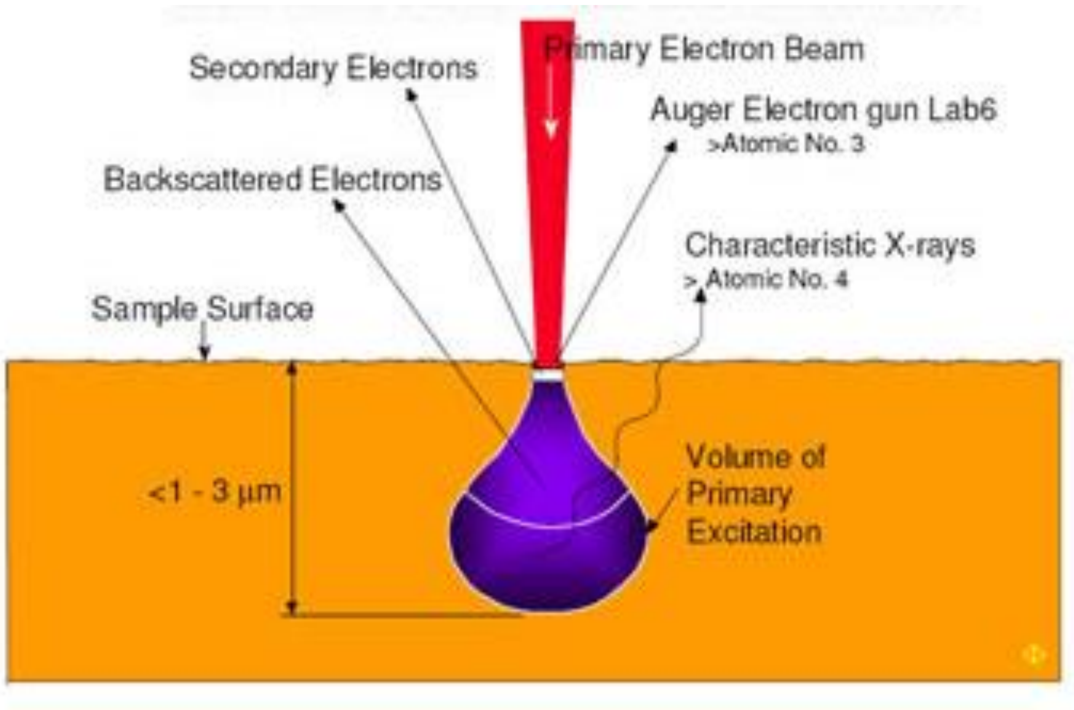

Figure 3 Schematic drawing of the electron beam sample interaction [2]

Backscattered electrons (BSE) are beam electrons which have undergone an elastic interaction with the sample surface, and have experienced a high angle (≈180°) change in trajectory. Thus, these electrons are scattered back towards the beam source. This signal contains a limited amount of topographic information but is extremely sensitive to the average atomic number of the sample surface, a type of compositional information.

Finally, a certain number of beam electrons will essentially be conducted by the sample to ground (Figure 4) [3], and this measurable current is termed specimen current (SC). The SC signal reflects changes in both the SE (due to topography) and BSE (due to compositional variations) signals and can therefore be used to construct microscopic images of a sample surface which contain both topographical and compositional information.

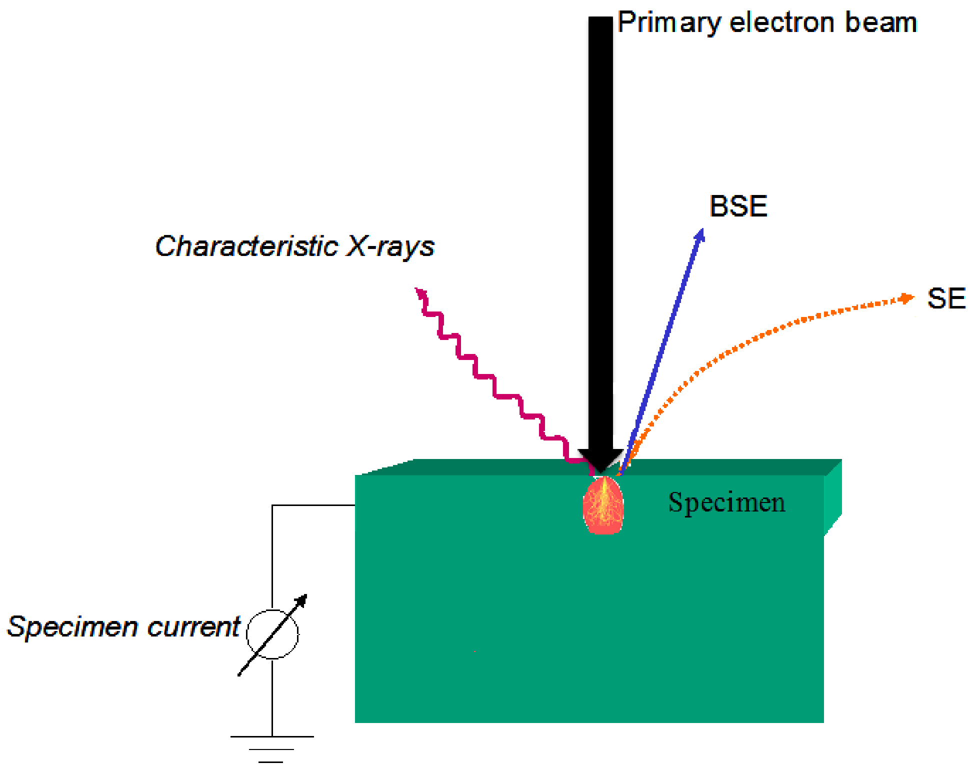

Figure 4 Schematic drawing showing specimen current (adapted from [3])

In e-beam instruments like the SEM and EPMA, resolution should not be confused with magnification. Resolution is largely decoupled from magnification, unlike in optical microscopy. Hence, it is possible to have higher and higher magnification images of a region of interest (ROI) with no increase in resolution, a phenomenon known as empty magnification. The resolution in an e-beam instrument is determined by the minimum spot size of the electron probe (d_p) and the dimensions of the interaction volume (Figure 9) [4] created when an electron probe impinges on a sample surface.

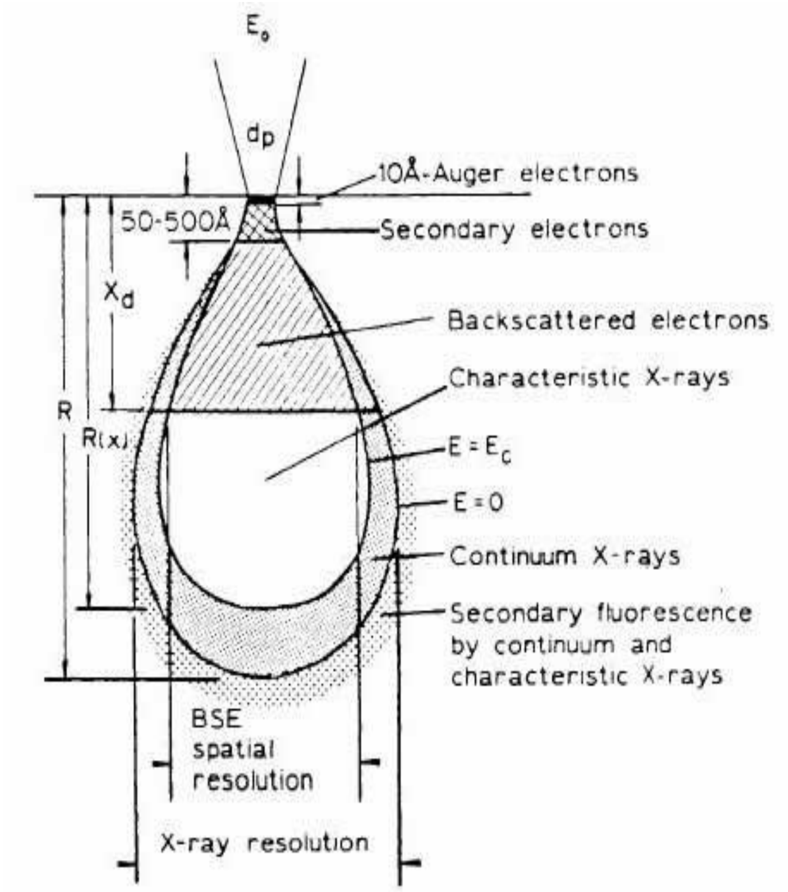

Figure 5 Schematic drawing of the interaction volume [4]

The interaction volume is nominal tear-drop or pear shaped with a lateral-spatial diameter of ≈1µm. Secondary electrons have very low energies (≤ 50 eV) and consequently are only able to escape from the first few nanometers of the sample surface. They are very sensitive to the sample surface topography and are therefore, used to construct high-resolution (<10 nm) topographic images.

Backscattered electrons have energies on the order of the e-beam probe (KeV) and can therefore escape from much deeper portions of the interaction volume. Also, due to their much higher energy BSE can emanate from areas much farther away from the beam impact point compared to SE and consequently can be used to construct images with far more limited resolution.

The characteristic x-ray signal can originate from regions much more deeper of the sample compared to the BSE signal and can only be used to construct images with a nominal resolution close to the dimensions of the interaction volume (≈1μm). In summary, while the SE signal can be used to construct images of the sample surface topography with resolutions of <10nm, the BSE and characteristic x-ray signals can be used to generate compositional images with lower lateral-spatial resolutions, much poorer than that of SE images. Finally, given that the average atomic number of cementitious materials is of relatively low atomic number (Z) (compared to say a pure metal or alloy); the resolution of compositional images of these materials is likely worse than ~1μm.

The other most important signal generated from e-beam-sample interaction is “light” in the form of x-rays. The x-rays are both continuum and characteristic; the continuum x-rays are produced via deceleration of beam electrons as they experience coulombic interactions with the electron clouds and nuclei of sample atoms and can therefore have any energy up to that of the beam energy. These x-rays do not provide information about sample composition.

Characteristic x-rays are generated by inner electron shell ionization of sample atoms by the e-beam; the ionized atoms undergo a relaxation process in which electrons from higher shells drop down to fill the voids left in inner-shell ionizations. This transition from “high” shell to “lower” shell is accompanied by the emission of an x-ray of a specific energy, characteristic of the type of shell-to-shell transition. The energy, wavelength and pattern of these transitions are very unique to each element and can therefore be used to identify and quantify the element composition of the sample surface interacting with the e-beam.

Most elements actually emit an associated family of x-ray lines with increasing amounts of lines for increasing numbers of electrons and electron shells. A specific line of the family of lines emitted from one element can overlap with a line of other element thus complicating the unambiguous identification and quantification of elements present in complex samples. These lines have been extensively characterized over the years and are commonly available in built-in electronic identification tools.

In an EDS system, x-rays emitted from the sample with an appropriate trajectory are collected by a small diameter biased disc of SiLi (silicon-lithium) diode cooled by liquid nitrogen (Figure 6) [1]. The x-rays create electron-hole pairs in the SiLi diode detectable as a voltage; the number of hole-pairs i.e., the voltage is proportional to the absorbed x-ray. Through a series of electronics and processing, single x-ray absorption events (voltage pulses) can be quantified and displayed in a spectrum of counts as a function of energy (usually KeV). Indexing (assigning the peaks in the spectrum) allows for identification of the elements in the ROI.

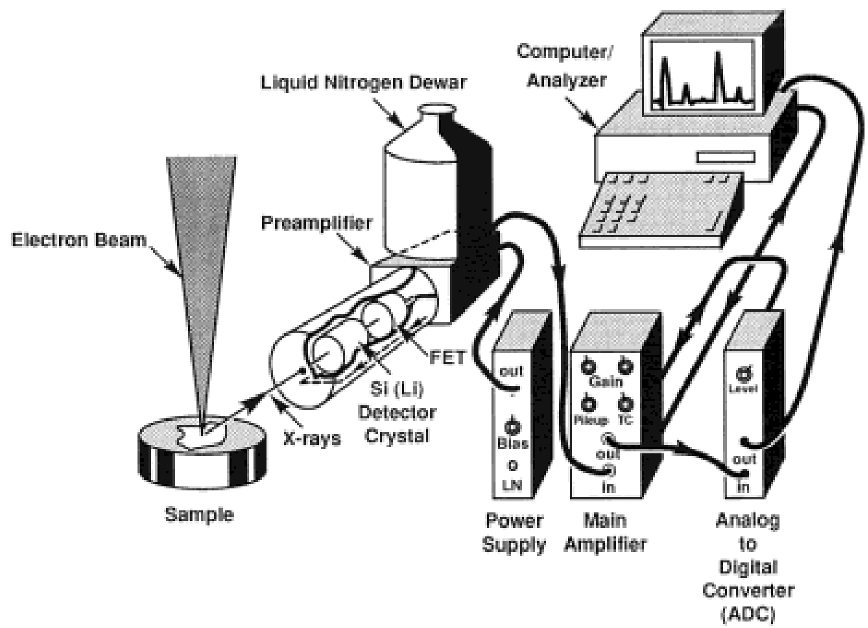

Figure 6 Schematic representation of an energy-dispersive spectrometer and associated electronics [1]

In a WDS system sample-emitted x-rays with appropriate trajectories enter the detector. They impinge first on a near-prefect crystal with a specific d-spacing and orientation. X-rays with specific wavelengths hitting the crystal at Bragg angles are diffracted at known angles. A simple gas-filled detector (gas proportional counter) placed at a specific position with respect to the crystal and the sample, called Rowland circle geometry, serves as an x-ray detector (Figure 7) [1].

The detector has a wire with a strong positive bias; incoming x-rays ionize the gas; the electrons produced are accelerated toward the positively biased wire. These electrons produce a wave of secondary ionization and all of these electrons are collected by the wire and generate a current in the wire that is converted into voltage pulse. This detector is tunable, with the crystal acting as a sort of x-ray band pass filter (Figure 8) [1].

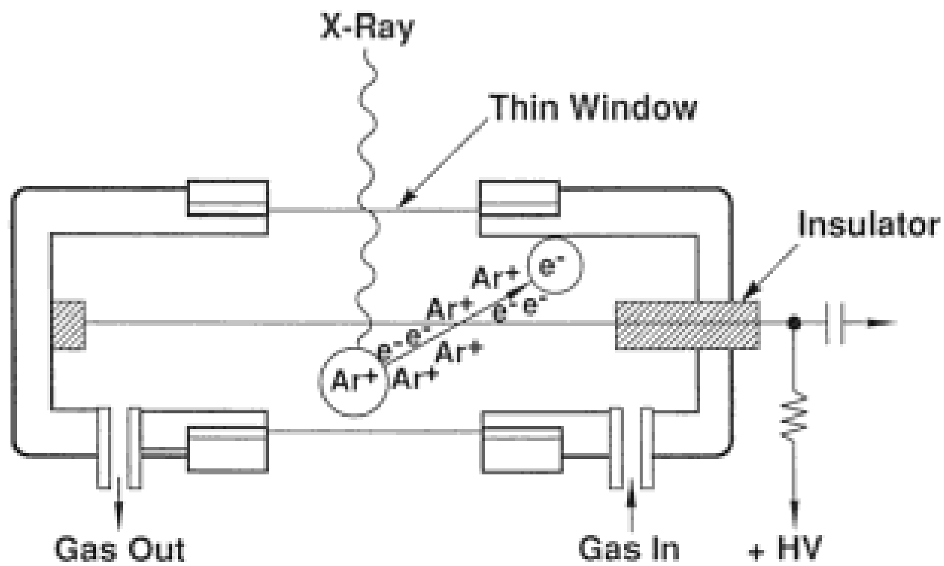

Figure 7 Schematic drawing of a gas flow proportional counter [1]

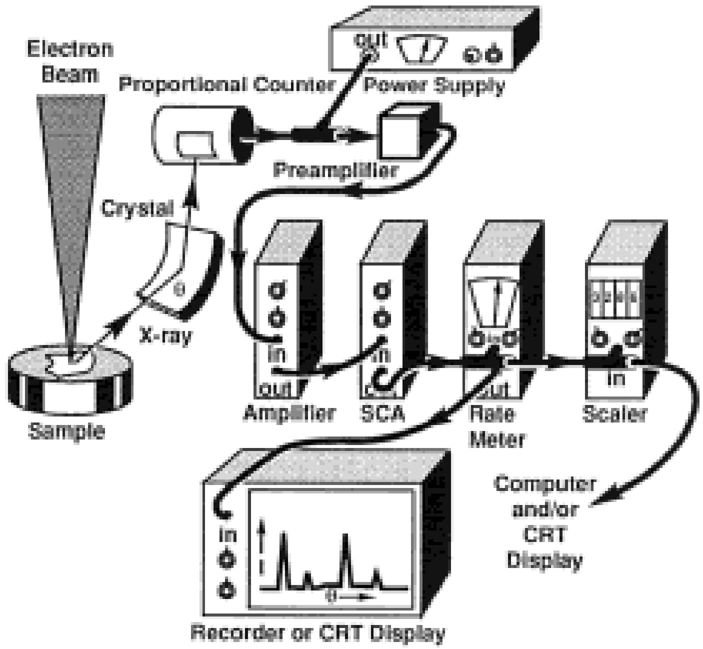

Figure 8 Schematic representation of a wavelength dispersive spectrometer and associated electronics [1]

The WDS system has higher spectral resolution (~5eV) than the SiLi diodes employed for EDS. Because probe currents orders of magnitude greater than that used for EDS are required, WDS x-ray count-rates are much larger. Both of these strengths contribute to the 10 times order of magnitude improvement in the lower limit of detection for many elements (particularly low atomic number elements) compared to EDS. In WDS collections, great care is given to maintain the beam normal to the sample surface and for making the surface flat via polishing, with a mirror finish and average surface roughness of ≥1μm.

Keeping the beam normal to the surface maintains the Rowland circle geometry; average roughness orders of magnitude greater than this have an impact on the detected signal, resulting in poorer limits of detection. These same issues are important to quantitative EDS, however, most EDS collection are typically semi-quantitative at best.

It is important to understand the digital nature of all image data generated from an SEM or EPMA. All these images are essentially signal intensity maps; the maps are composed of picture elements (pixels) which link the signal intensity at a physical location on a sample surface with a position in the image (figure 9) [1]. To create an image, the electron beam is addressed to a specific spot on a sample for a finite length of time (dwell time) and the various signals are detected and counted. Following a pattern of predetermined rows and columns, the beam is addressed to another spot on the sample and the signal intensities recorded. This process is repeated until the entire array has been covered.

In both the SEM and EPMA, the beam itself can be scanned to each spot of the pattern, or the sample can moved under a fixed beam essentially normal to the surface. Imaging a relative small area (several hundred μm^2) can be achieved by scanning the beam. However, since the beam can only be deflected through a small distance, imaging of large areas (mm^2 and cm^2 in area) requires the stage to move, so called “stage rastering”, to cover each spot/pixel in the array.

Magnification in this type of imaging follows the relationship of scan area/screen area. Dimensions and numbers of pixels on the video screen/monitor, in our instruments a cathode ray tube (CRT), or captured digital image are constant. The number of pixels and their relative lateral-spatial relationship with each other matches those of the CRT (1:1 correspondence); however, the pixel dimensions resulting from scanning the beam in an array on the sample surface change depending on the length and width of the scan array. Therefore, if for example it is assumed that the typical CRT pixel dimensions are 100 μm x 100 μm and the typical screen size is 10 cm. x 10 cm., scanning the e-beam on the sample surface in the 1:1 scan array with pixels 10 μm x 10 μm in size yields a scan area of 1cm x 1cm and a resultant magnification of 10X. Higher and higher magnifications (up to 1,000,000X in some of today’s best instruments) can be achieved by scanning increasing smaller areas composed of increasingly smaller scanned pixels.

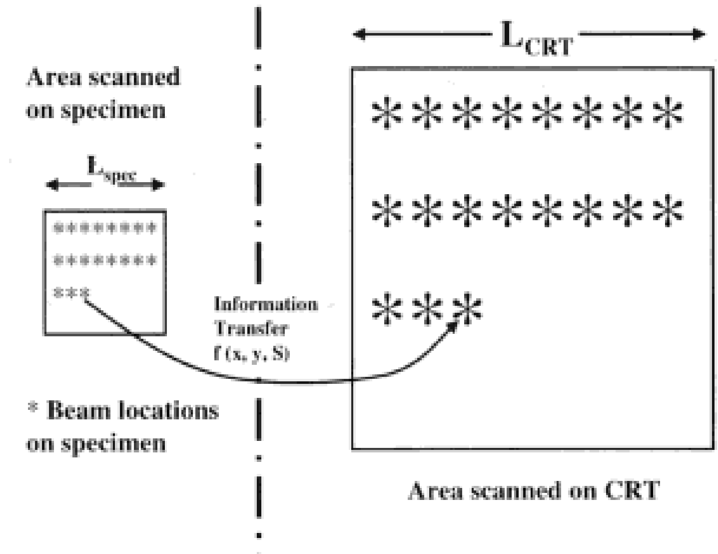

Figure 9 Principle of image display by area scanning [1]

X-ray maps consist on arrays of pixels (dots) that indicate the presence of a specific/selected element in a specific location on the sample, typically corresponding to the size of the interaction volume. The maps, usually qualitative in nature, provide an element distribution across a ROI that can be overlapped with topographical (SE) or compositional images (BSE).

CHAPTER 3
METHODOLOGY

Experimental Design

All samples studied in this report were prepared and received from FDOT-SMO. This report was focused on two standard series called 1-series and CFS-series, and the three provided concrete samples from FDOT-SMO Cl ion diffusion experiments: B-15, E-15, and I-15. All samples were saw cut by FDOT-SMO with a large tile saw. 1-series consisted of 13 samples of cement-only (w/c = 0.3) mixed with known amounts of NaCl in an added concentration range of 0.01 – 1.0 wt. % Cl. The CFS series consisted of 13 samples that were cement (w/c = 0.3) containing a constant amount of fly-ash and sand plus known amounts of NaCl ranging from 0.01 – 1.0 wt. % Cl. The data corresponding to the 1-series and the CFS series can be found in the appendix (Tables 2 and 3).

All samples in both standard series were initially cast into cylindrical molds (10.16 cm length, 4.32cm diameter). After pouring into mold samples were spinned for the first 24 hours. Samples were cured additional 27 days in the mold and then demolded. The total cure age was 28 days. After demolding the samples were sliced removing two one inch (2.54 cm) sections, one from the top and one from the bottom (see figure 10a), leaving the middle section to be used in this study. The samples were then bifurcated parallel to the cylindrical axis to produce two samples with rectangular fronts and half-cylinder backs (figure 10b).

The rectangular face of each standard then needed to be ground level (down past any marks or damage left by the saw) using a very course polish paper and polishing wheel or a grinding stone. Each standard then need to be polished to a mirror-finish (scratches < 1μm) or as close as possible to satisfy the geometrical constraints described above.

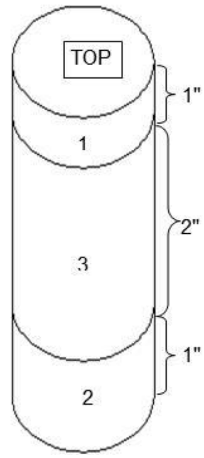

(a)

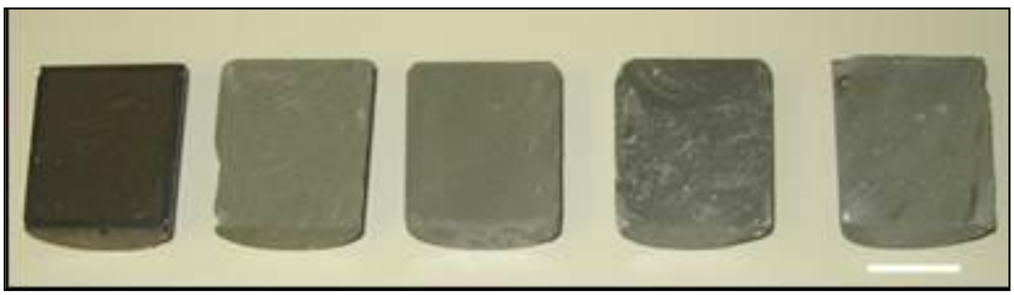

(b)

Figure 10 (a) Sectioning of cement samples, (b) Cement samples with rectangular fronts and cylindrical backs (scale bar 2.54 cm)

The rectangular face of each standard then needed to be ground level (down past any marks or damage left by the saw) using a very course polish paper and polishing wheel or a grinding stone. Each standard then need to be polished to a mirror-finish (scratches < 1μm) or as close as possible to satisfy the geometrical constraints described above. Because they consisted only of cement and were relatively soft, 1-series standards were polished by hand at MAIC using a Buehler polish wheel and polish papers over a range of grits down to < 1μm. The very first samples were polished using kerosene as lubricant; use of water, some alcohols and acetone should be avoided as these can solvate Cl and leach Cl form cementitious sample surface and bulk.

However, polishing in kerosene had many drawbacks and permanently impregnated the samples with kerosene, so its use was quickly abandoned in favor of a draw-polishing method. In this method, still conducted under a fume hood, no lubricant was used. Instead, the polishing papers were replaced more frequently and debris on the samples was cleared using regular blasts of compressed nitrogen or argon from a triggered hose nozzle. Dust was regularly cleaned up with water, damp paper towels, and put into a covered waste bucket for environmental health and safety (EH&S) disposal; polishing papers were also soaked in water before disposal to maximize dust containment and minimize dust exposure. Though this method yielded excellent 1-series samples, it was extremely time consuming and not cost effective. It could also not be used for the CFS series or any of the experimental samples as they were much harder than the 1-series samples and destroyed or could otherwise not be polished by hand using a wheel and paper.

All other samples were therefore sent to American Petrographic Service, INC. (APS) (St. Paul, MN), and were prepared and polished by Christopher Owen. Among other services, APS has dedicated sample preparation facilities including robust sample preparation instruments such as large stone grinding wheels and dust scavenger systems. The experimental samples B15, E15, and I15 were cut into rectangles by FDOT-SMO, and were then polished by APS.

The sample preparation methodology used by APS is as follows:

- Samples are received and unpacked.
- Approximate dimensions of sample batch are recorded.
- Sample identification is observed and labeling of samples is confirmed or applied, if necessary.
- A dry, magnetic, diamond abrasive mat is applied to a lapidary wheel.
- Wheel is engaged.
- Sample is held, saw-cut surface down, on the abrasive surface.
- Compressed air is used as needed to clear dust build-up off abrasive mat

and sample surface.

- Sample is ground with progressively finer abrasive mats until a smooth matte finish is achieved. Grits used: 80, 220, 600, 1200
- Compressed air is again used to clear dust build-up off sample surface.
- Once all samples are polished, they are re-packaged in clean bags and shipped to University of Florida for examination.

All samples (standard and experimental) were blown off with compressed gas and stored in vacuum desiccators at a rough vacuum. The samples were stored for at least two weeks under this vacuum which removed water resulting essentially in drying the sample surfaces. Before any sample was properly analyzed by either the SEM or EPMA, the surface to be analyzed was rendered conductive. This was required because a significant portion of the e-beam is deposited into the sample and charge builds up in the sample if the analyzed surface is not conductive and a good path to ground (instrument stage) is not maintained.

For high dielectric (non-conductive) materials like cement and concrete, a thin conductive film (typically carbon or gold) coating is applied to the surface to be studied. For x-ray studies, carbon is used because it does not generate x-rays that overlap the x-rays of interest from the sample. All samples were coated as follows: using conductive carbon paint, a ≈ 6mm. thick border was painted on all the edges of the polished surface and then all the way down to the corresponding four sides. Once all the paint had dried in open air, the sample was placed into the bell jar of an evaporated-carbon sample coater. After achieving a high vacuum in the bell jar, a high current was applied across a thin carbon rod which generated an arc, thereby evaporating the carbon rod. A thin amorphous layer of carbon deposits on everything (including the polished sample surface); the sample is additionally rotated in the chamber during arcing to achieve a more uniform sample coating. Once coated, samples were ready to be loaded into the instruments. It is important to mention that the use of epoxy-impregnation was completely avoided for all samples; though there are purportedly low Cl epoxies available, they are expensive and not widely available. Finally, epoxy impregnation provides only a dubious advantage, at best, to improving the quality of the analysis.

Equipment

The scanning electron microscope used in MAIC was a JSM-6400 equipped with an Oxford Link Isis imaging-EDS hardware, and Windows software as well as a Deben Sprite 2-axis (X and Y) programmable motorized stage. In order to conduct large scale SEM x-ray mapping studies, a custom piece of Windows software interfacing the Deben Sprite programmable stage and the Oxford x-ray mapping software was needed and written by Richard Deist.

The EPMA used was a SuperProbe JSM-733 equipped with a Tracor-Northern WDS hardware and custom (non PC) software package including a programmable motorized 3-axis stage. Collection of large-scale x-ray maps from the microprobe was more complex and also required custom Window-based software to be created. All custom software and macros created for this project are provided in a supplemental electronic file archive.

Procedures

For SEM-EDS the size/pattern of the large-scale collection was programmed using an A-Stage and an array (< 200) of x-ray maps (50X) were collected using the speedmap feature in the Link-Isis software. The elements collected for mapping were predefined by custom energy windows created over discrete energy ranges (KeV) on the EDS spectrum. Forty repeated frames were collected simultaneously for each element of interest including silicon (Si), calcium (Ca), chlorine (Cl) and aluminum (Al); and a backscatter image was also collected for each spot in the mapping array.

After completing a full collection on a sample (≈8 hours), another software utility then converted all of the individual maps into TSV (tab-separated variable) image files from the proprietary Link-Isis format. This format is a general imaging format that can be imported into ImageJ, a powerful free image processing and analysis software developed by the National Institute of Health (NIH) that will be discussed in more detail later in this section.

For EPMA-WDS the software developed (AutoProbe) was even more robust. Working through the 5500 and 5600 Tracor-Northern hardware and that proprietary software/language, AutoProbe coordinated the collection from a Windows PC over a serial connection of large arrays of points (<100,000). AutoProbe assembled all these points into x-ray maps in real-time. In addition to the four elemental x-ray maps, a specimen current map was also constructed. The probe was equipped with four spectrometers thereby enabling the simultaneous collection of four different elements. We therefore collected calcium (Ca), silicon (Si), chlorine (Cl), and sulfur (S). Large collections took > 30 hours due mainly to the limited speed of the serial connection, the PDP11 hardware used in the Tracor-Northern stand-alone, and the 100 ms. dwell-time minimum limit built into the proprietary 5500 software. Specific key operating details used for both instruments during all collections are summarized in Table 1.

ImageJ software was used extensive throughout the project to process the large amounts of image data into quantitatively meaningful images and graphics. Software macros developed by Rick Diest were therefore created to facilitate the import and conversion as well as the assemblage of the data from the Link-Isis system and from the AutoProbe software.

Table 1 Operating parameters used for SEM and EPMA

SEM-EDS	
□	Probe Current: 9 nA (~20% dead time)
□	Resolution: 26.78 pixels/mm *(~37 μm effective step)*
□	Accelerating Voltage: 10 kV
□	*Dwell Time: ~20 ms (<u>rough</u> approximation)*
□	Avg. Collection Time: 17.5 sec/mm^2
□	Detector Mode: “Optimum acquisition rate”
□	Speedmap frames: 40
EPMA-WDS	
□	Probe Current: 200 nA
□	Resolution: 10 pixels/mm (100 μm step)
□	Accelerating Voltage: 15 kV
□	Dwell Time: 200ms
□	Avg. Collection Time: 86.1 sec/mm^2

The best opportunity for quantifying the concentration of a single element in an extremely complex and heterogeneous matrix like cementitious materials using the SEM or the EPMA is to construct what is known as a calibration curve, or series tallying the x-ray counts from standard samples with various known Cl concentration levels. Ideally to construct such a calibration curve, standard samples, exactly the same in composition to the experimental to be investigated, are prepared with increasing known amounts of the analyte (Cl in this case). Fortunately, with cement and concrete mixes, this is easily possible.

This was indeed the approach implemented by Mori et al. and was therefore adopted for this study. Mori et al. also made a very strong case that separating the paste pixels from those that are aggregate, and conducting the study profiling only the paste for Cl, yielded Cl concentration results more closely matching to those generated by wet chemistry. This follows from the primary assumption that Cl diffuses essentially only through the paste, and paste makes up only a fraction of most concrete. Therefore, the x-ray maps constructed using e-beam methods were composed largely of pixels corresponding to large (rock) and small (sand) aggregate. Since this rock and sand aggregate contain very low amounts of Cl, if any, their corresponding pixels have very low if not zero Cl x-ray counts. If these Cl x-ray counts are included as well as the counts from paste pixels to calculate the average Cl x-ray counts for a given area of concrete, the average can be significantly impacted by the inclusion of large numbers of essentially zero Cl x-ray counts from aggregate pixels. This influence on the average Cl x-ray counts translates into potentially erroneous calculated values of the Cl concentration compared to wet chemistry measurements.

We therefore developed a paste-discrimination method based on imaging using a concept called pixel-masking or simply masking. In imaging, a mask can either preserve all pixels under the mask or exclude them; in this study the pixels under the mask we kept while all pixels not covered by the mask were set to a non-numeric value (not a number, NaN) which is analogous to turning these pixels off so that they do not show in the image and are excluded from any measurements made from the image. The paste-only mask must be generated from one of the other elemental maps or from some combination of them. An image with high contrast for paste pixels compared to aggregate is needed. Ideally, a mapped element other than Cl is found mainly in the paste at some relatively constant high level compared to the aggregate. This way, paste pixels that contain low levels or zero Cl are legitimately included in measurements and averages.

Calcium and silicon are not suitable because they are both found in paste; sulfur and aluminum (Al) however met this criterion. The S maps were therefore used to generate a paste-only mask for the probe data, and the Al for the SEM-EDS data. Thus, the data for the maps is obtained from the paste only. All pixels corresponding to fine and coarse aggregate are removed by the masking technique.

An example of the masking strategy described above can be seen in Figure 11; two areas of a concrete sample are shown: high and low Cl concentration. Our observations are that the polishing doesn't appear to smear anything since great care is taken during the polishing by cleaning the surface regularly with blasts of compressed air. In samples were a clear gradient is observed with wet chemistry, that gradient is also observed with our methodology. If there was smearing we should expect to see a random distribution of chloride or a homogenization of the chloride distribution on the surface. Even if there was smearing on the surface the data does not come from the surface, it comes from a several microns volume under the surface.

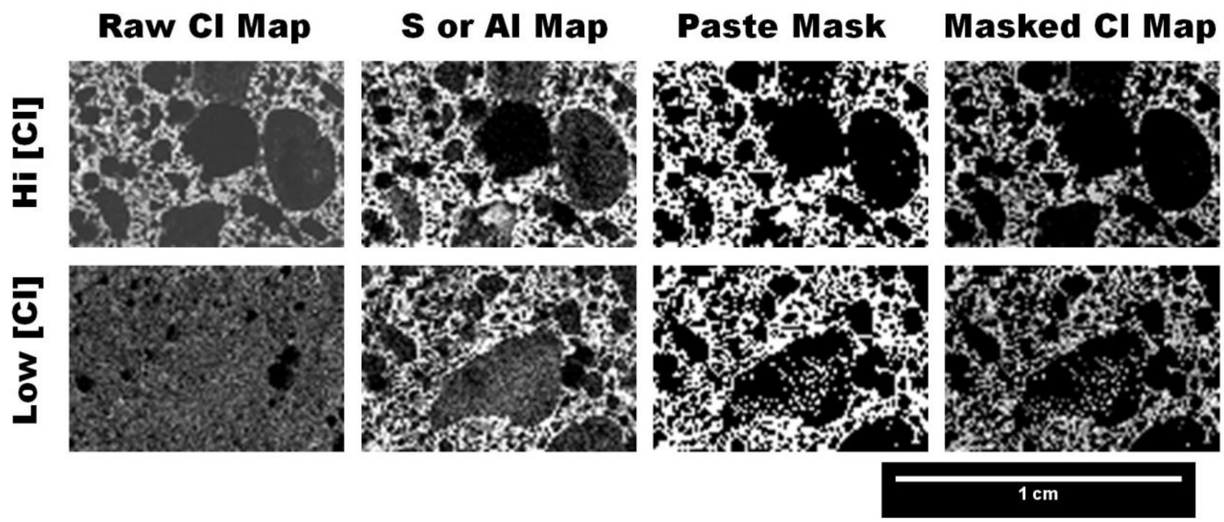

Figure 11 Example of the masking strategy showing high and low [Cl] areas

The calibration curves from the concrete samples were derived using a slight modification on the procedure that was applied to the standards. The paste-discriminated x-ray map was segmented into rectangular chunks, each representing a particular depth range from the exposed surface. These chunks were then quantified to allow plotting of X-ray intensity as a function of depth. To create a calibration curve, these depth/x-ray intensity data were plotted against the corresponding depth/Cl concentration data (from wet chemistry) provided by the FDOT and a linear regression equation was calculated relating X-ray intensity to Cl concentration.

CHAPTER 4
FINDINGS

Summary of Data

A summary of data can be found in Appendix 1.

Presentation of Results

Using EPMA-WDS paste-only Cl maps, master calibration curves for the 1-series and CFS standards were created (Figure 12); the corresponding Table 4 shows the raw data used to construct the curves as well as some descriptive statistics.

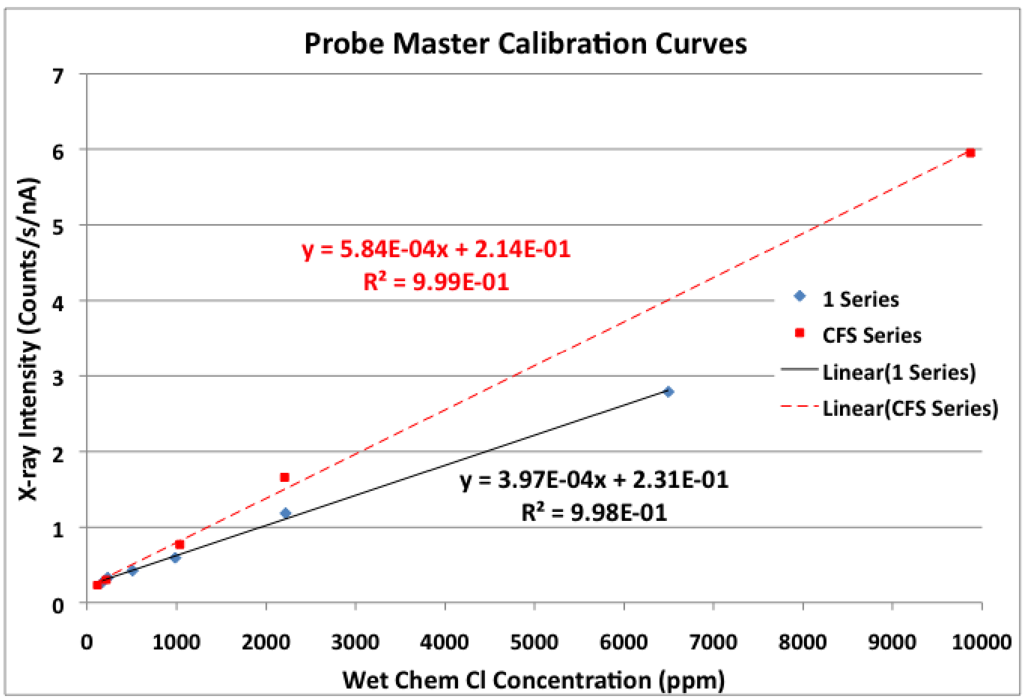

Figure 12 EPMA-WDS master calibration curves using paste-only Cl maps for the 1-series and CFS standards

Using SEM-EDS paste-only Cl maps, master calibration curves for the 1-series and CFS standards were created (Figure 13); the corresponding Table 5 shows the raw data used to construct the curves as well as some descriptive statistics (Table 6). The linear model fitted well all data sets collected on both instruments as evidenced by the coefficients of determination all nearly 1.

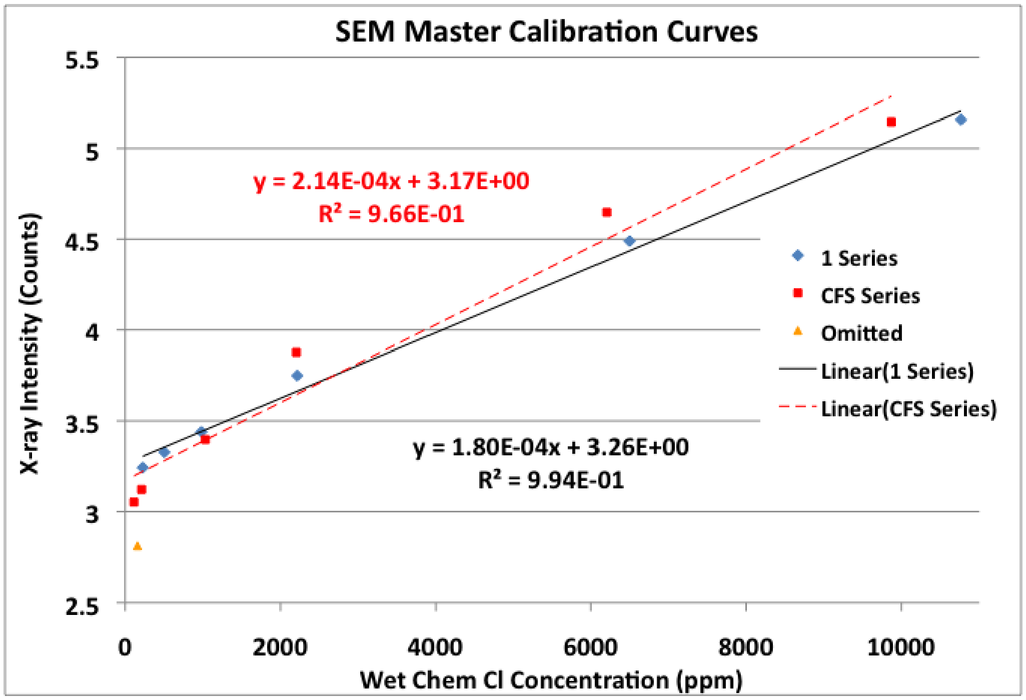

Figure 13 SEM-EDS master calibration curves using paste-only Cl maps for the 1-series and CFS standards

The following figures 14 to 19 show the linear and logarithmic calibration curves corresponding to samples B-15, E-15 and I-15 using tables 7, 8, and 9. Figures 20 and 21 (master calibration curves) combine correspondingly the linear and log curves for samples B-15, E-15 and I-15.

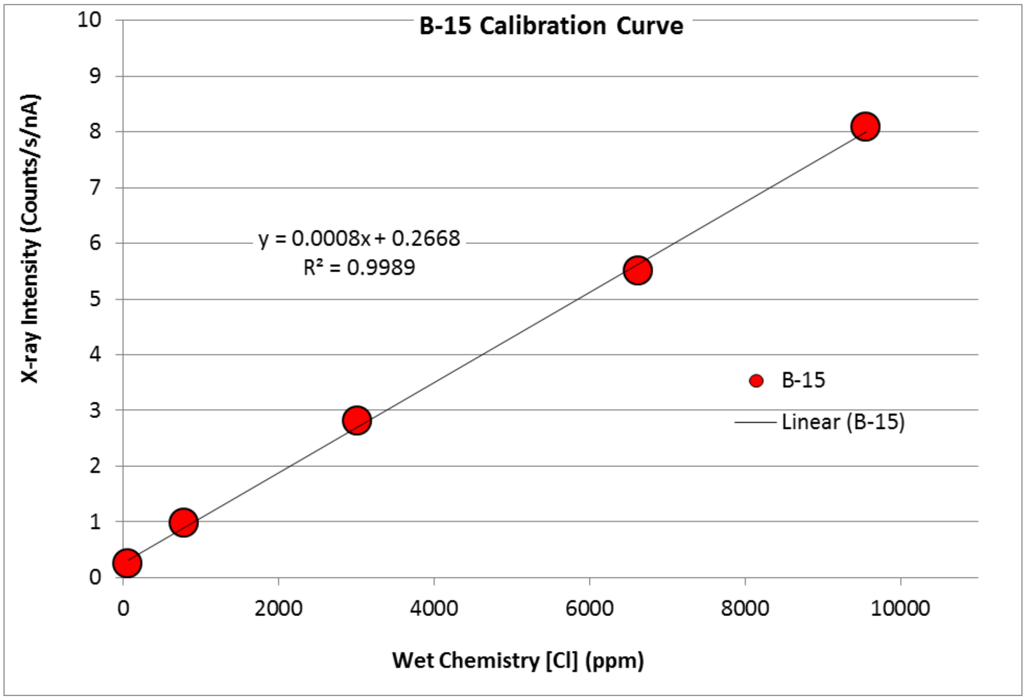

Figure 14 Calibration curve (linear scale) using paste-only Cl maps for the B-15 sample

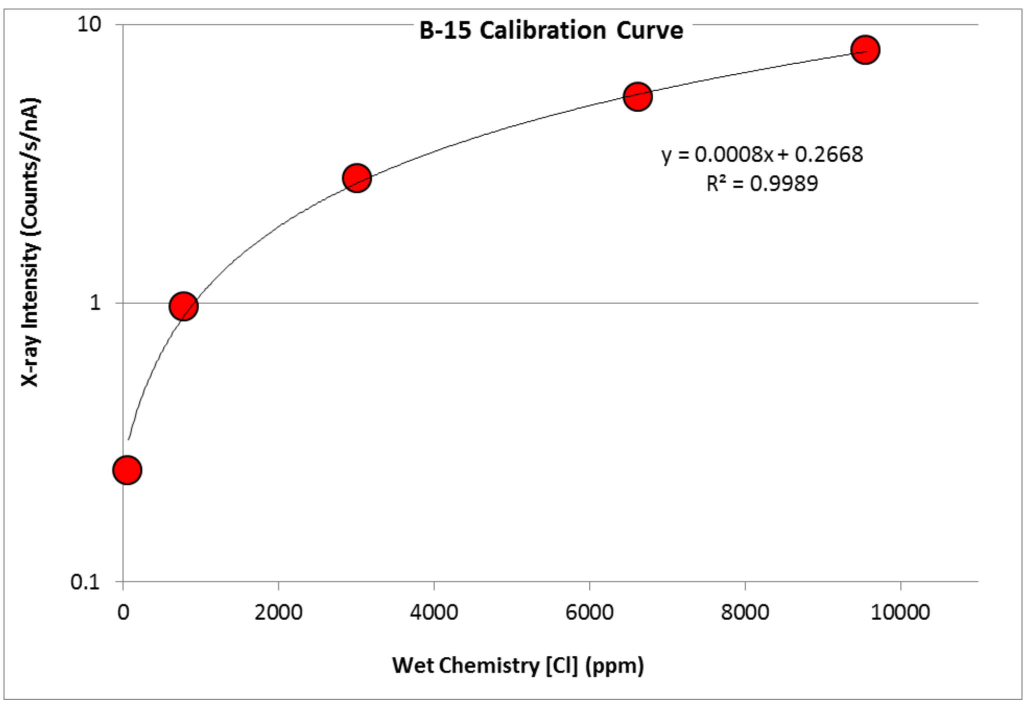

Figure 15 Calibration curve (log scale) using paste-only Cl maps for the B-15 sample

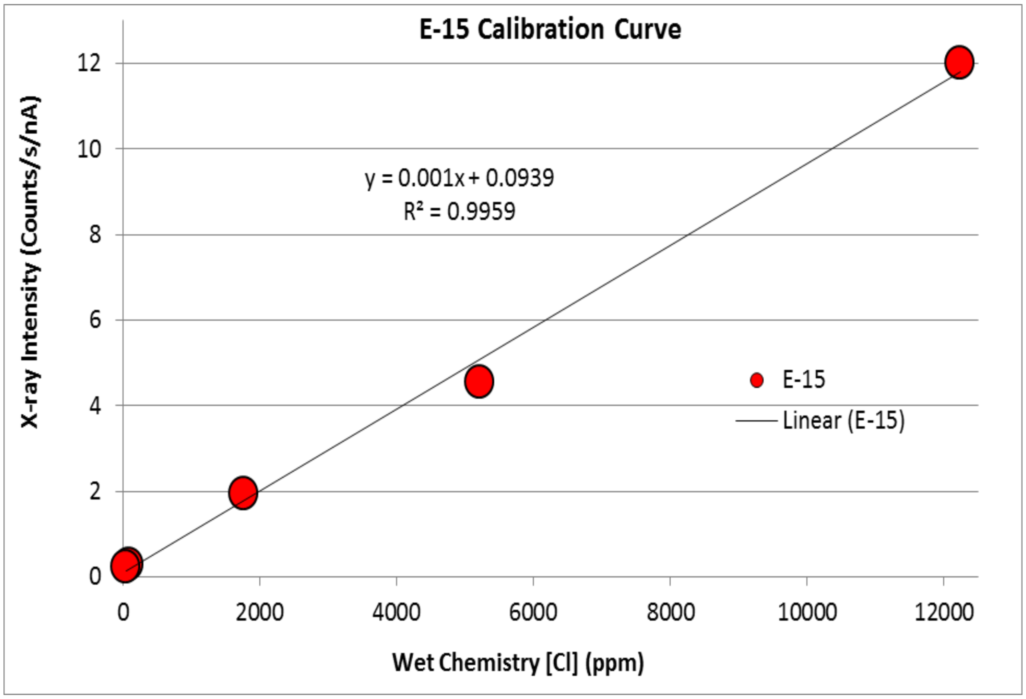

Figure 16 Calibration curve (linear scale) using paste-only Cl maps for the E-15 sample

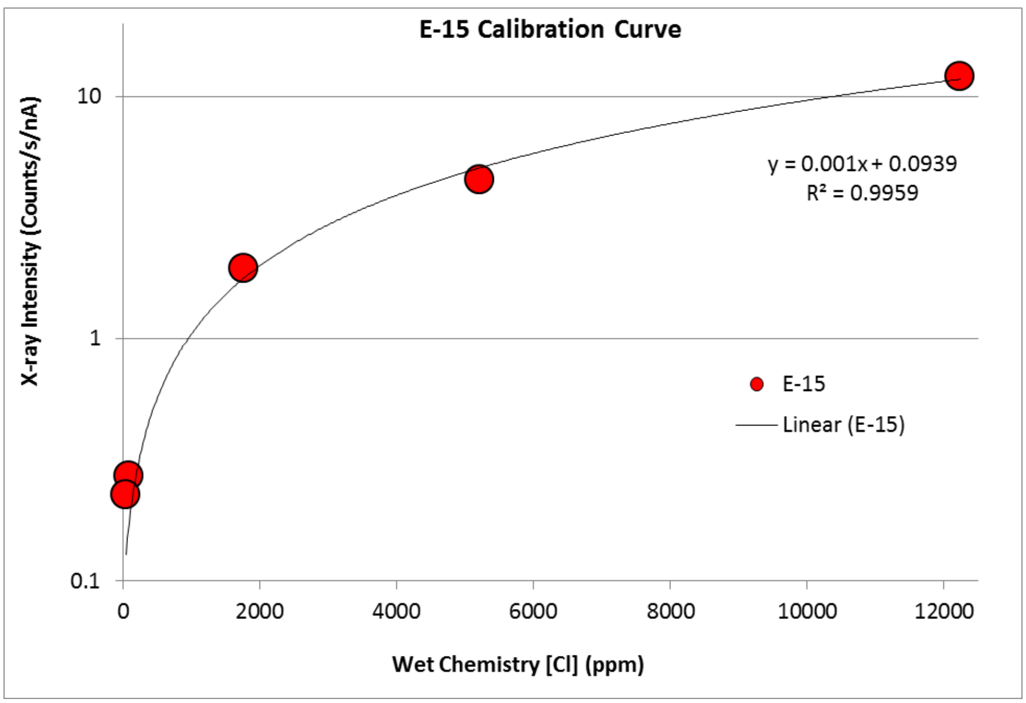

Figure 17 Calibration curve (log scale) using paste-only Cl maps for the E-15 sample

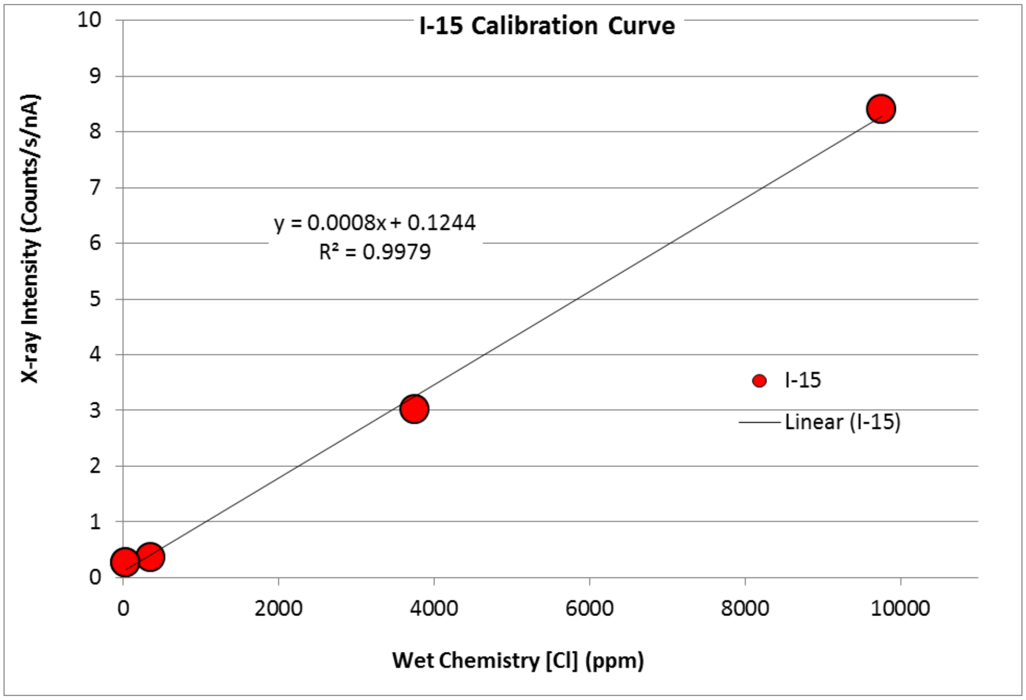

Figure 18 Calibration curve (linear scale) using paste-only Cl maps for the I-15 sample

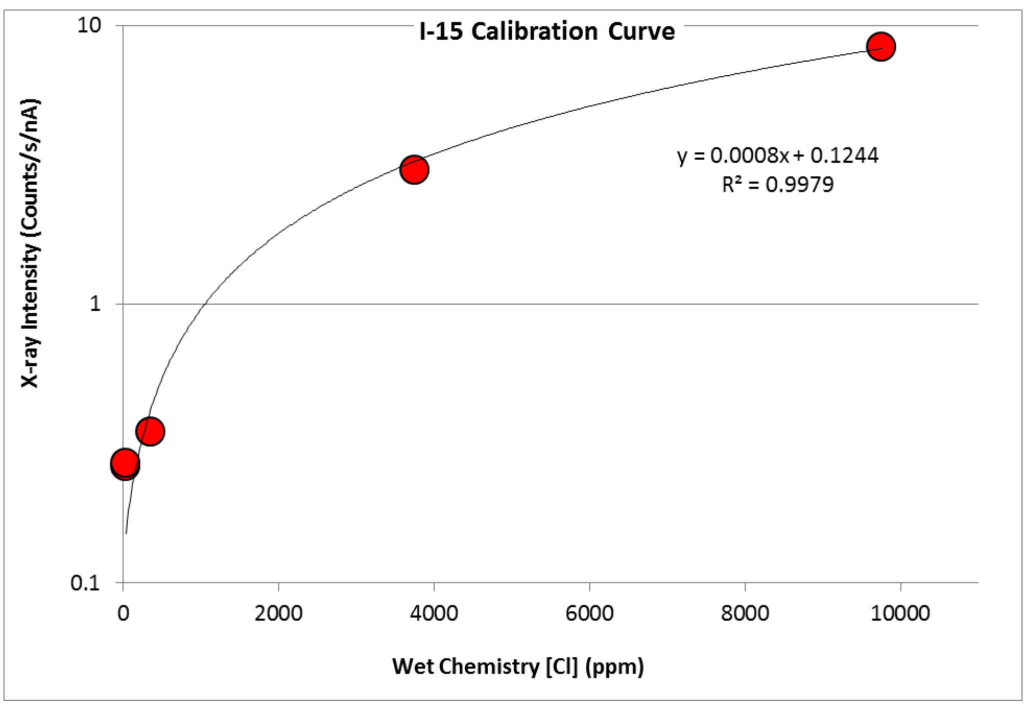

Figure 19 Calibration curve (log scale) using paste-only Cl maps for the I-15 sample

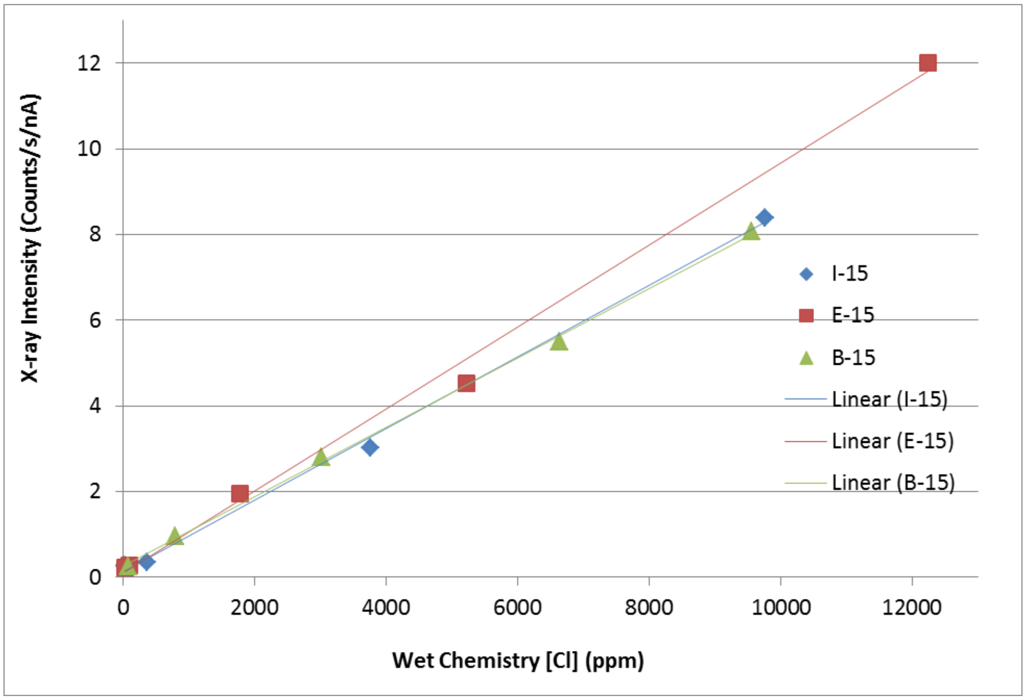

Figure 20 Master calibration curves (linear scale) using paste-only Cl maps for samples I-15, E-15 and B-15

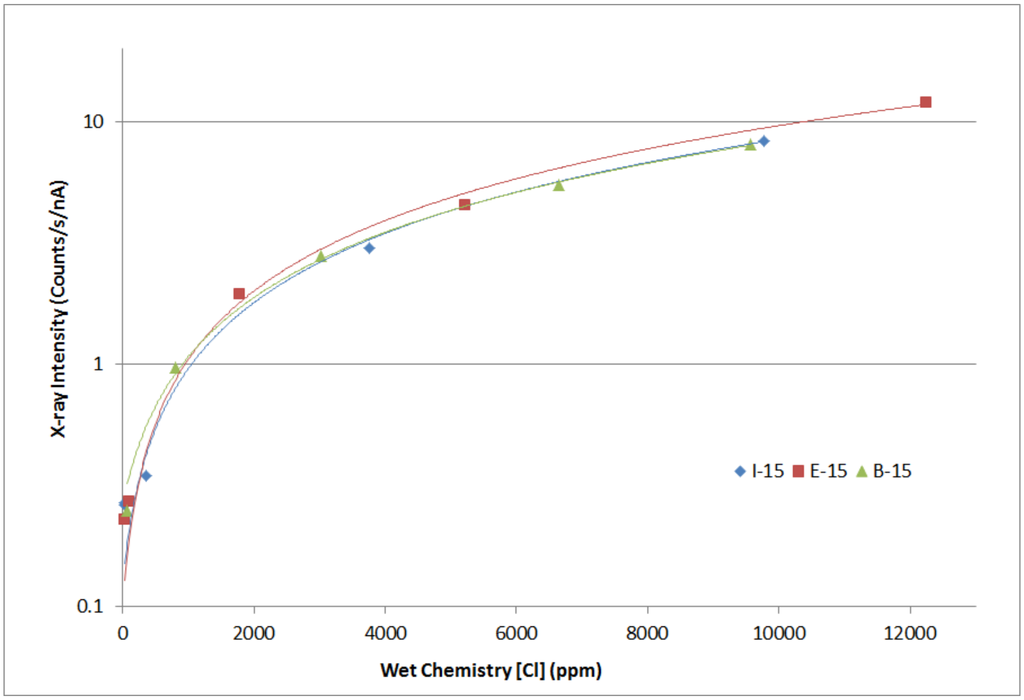

Figure 21 Master calibration curves (log scale) using paste-only Cl maps for samples I-15, E-15 and B-15

The following figures 22 to 36 show the results corresponding to the analysis of the concrete samples corresponding to diffusion experiments conducted at the FDOT-SMO.

The results corresponding to EPMA-WDS are presented for each experimental sample in Figures 22, 27, and 32 showing a specimen current image of the area being analyzed, a binary (black and white) paste pixel mask, and a paste-pixel-only Cl map. As explained previously, the specimen current provides an image that combines topography and average atomic number variations across the area analyzed. The rectangular areas of contrast correspond to separate data collection sessions. The paste pixel-only Cl map shows the distribution of Cl with a color code scale corresponding to the average count/s/nA that can be converted to concentrations using the regression equations obtained for the standards.

Figures 23, 28, and 33 correspond to the concentration depth profiles of samples B-15, E-15 and I-15. Figures 24, 29, and 34 correspond to the normalized depth profile obtained through the measurements done with EPMA-WDS. The intensities corresponding to the concentrations were normalized and are expressed in arbitrary units (AU). It is important to clarify that no correction factor was used to normalize the data. The normalization was achieved by taking the highest concentration or counts measured and dividing that set of data by that number. So it is not matrix or mix specific.

Figures 25, 30, and 35 correspond to the BSE imaging maps, binary paste pixel map, and paste pixel-only CL maps. The paste pixel-only Cl map shows the distribution of Cl with a color code scale corresponding to the average counts that can be converted to concentrations using the regression equations obtained for the standards. Finally, figures 26, 31, and 36 correspond to the concentration depth profile obtained through the measurements done with SEM-EDS. Again, the intensities corresponding to the concentrations were normalized and are expressed in arbitrary units (AU).

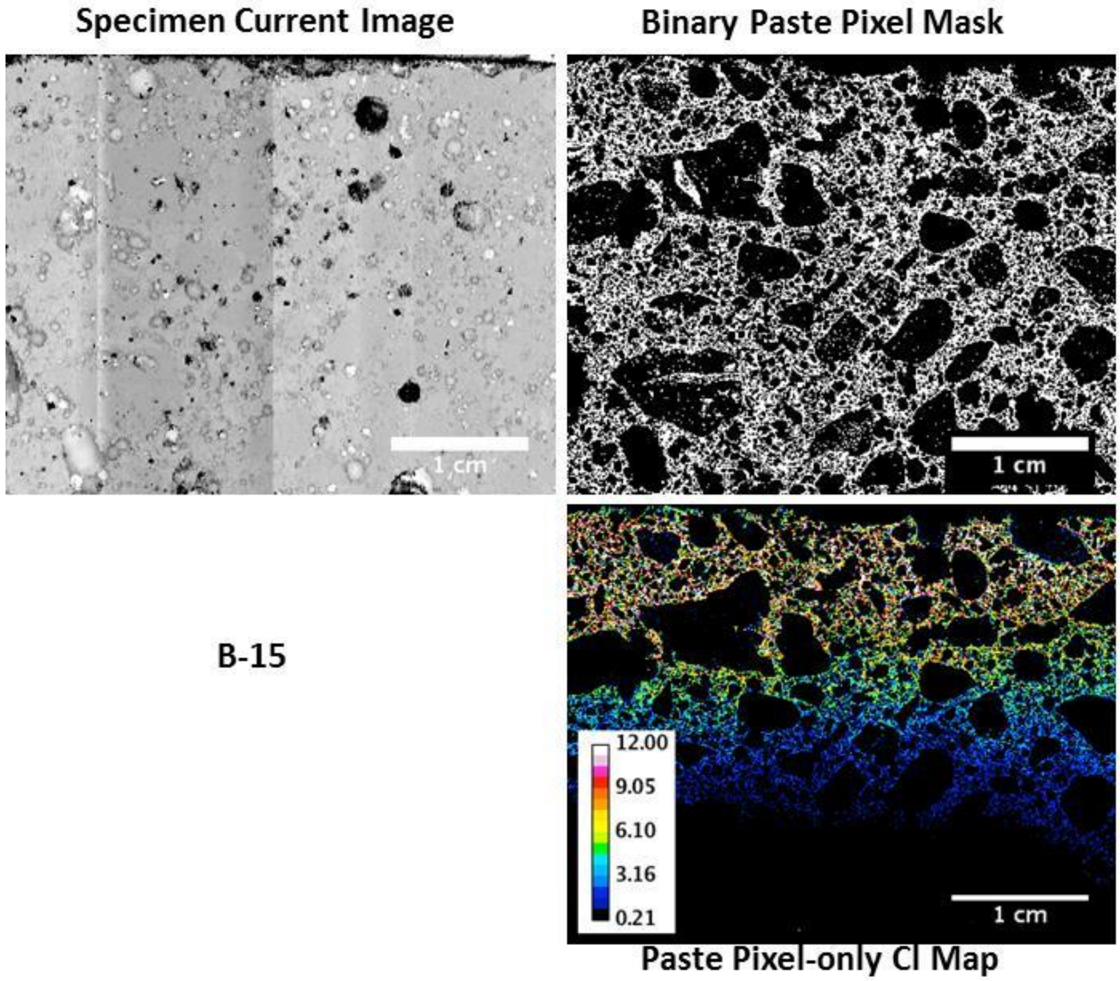

Figure 22 Specimen current image, pixel mask, and Cl x-ray map corresponding to sample B-15 using EPMA-WDS. Color code corresponds to Cl average count/s/nA

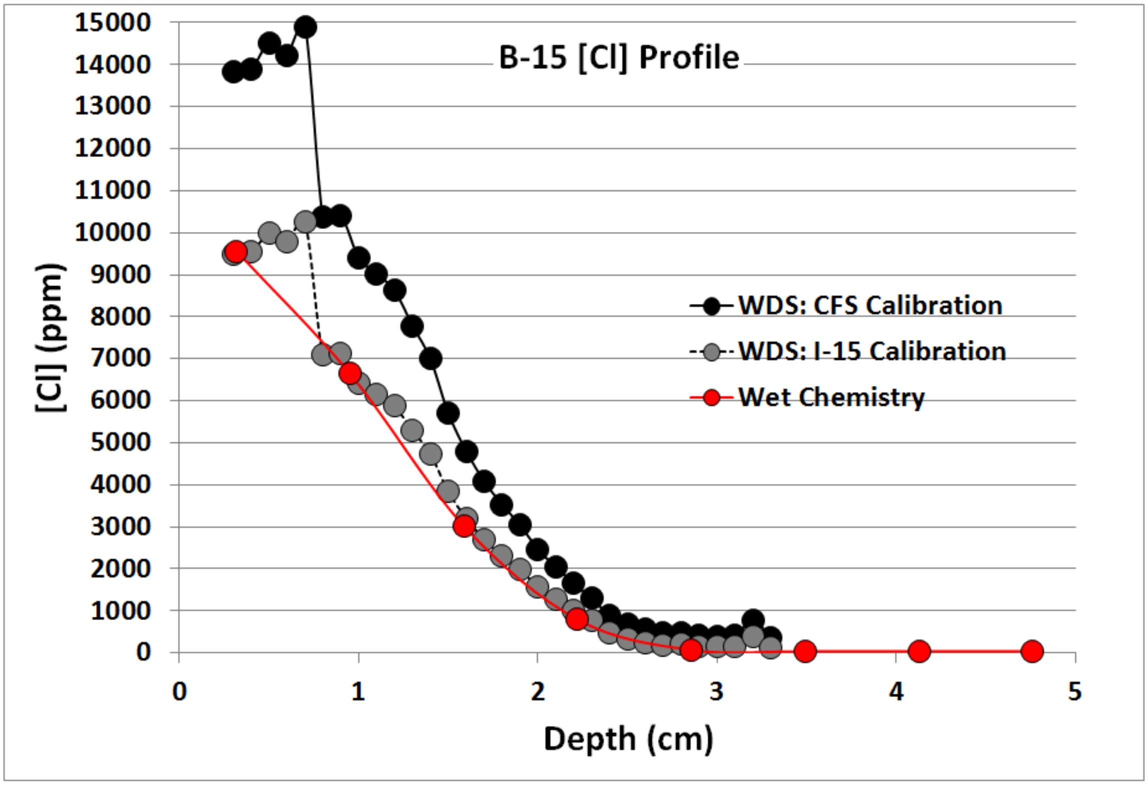

Figure 23 Concentration depth profile of sample B-15 with WDS

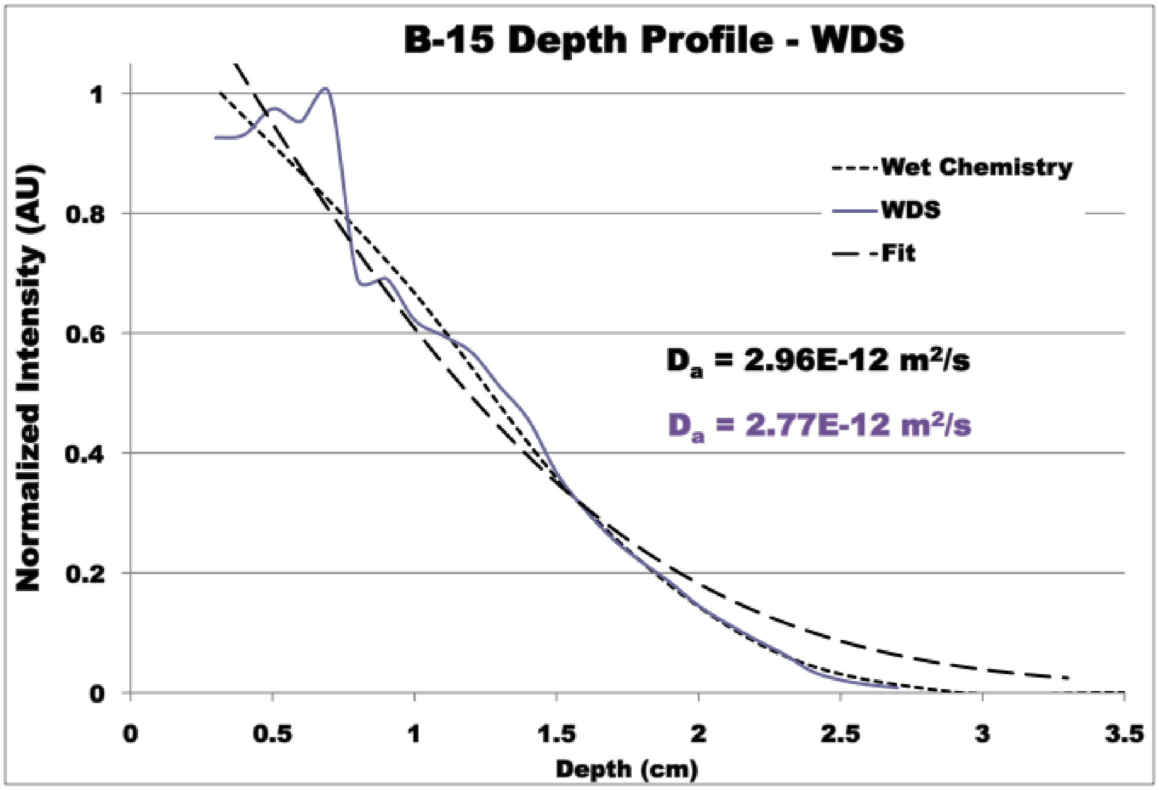

Figure 24 Normalized depth profile of sample B-15 with EPMA-WDS

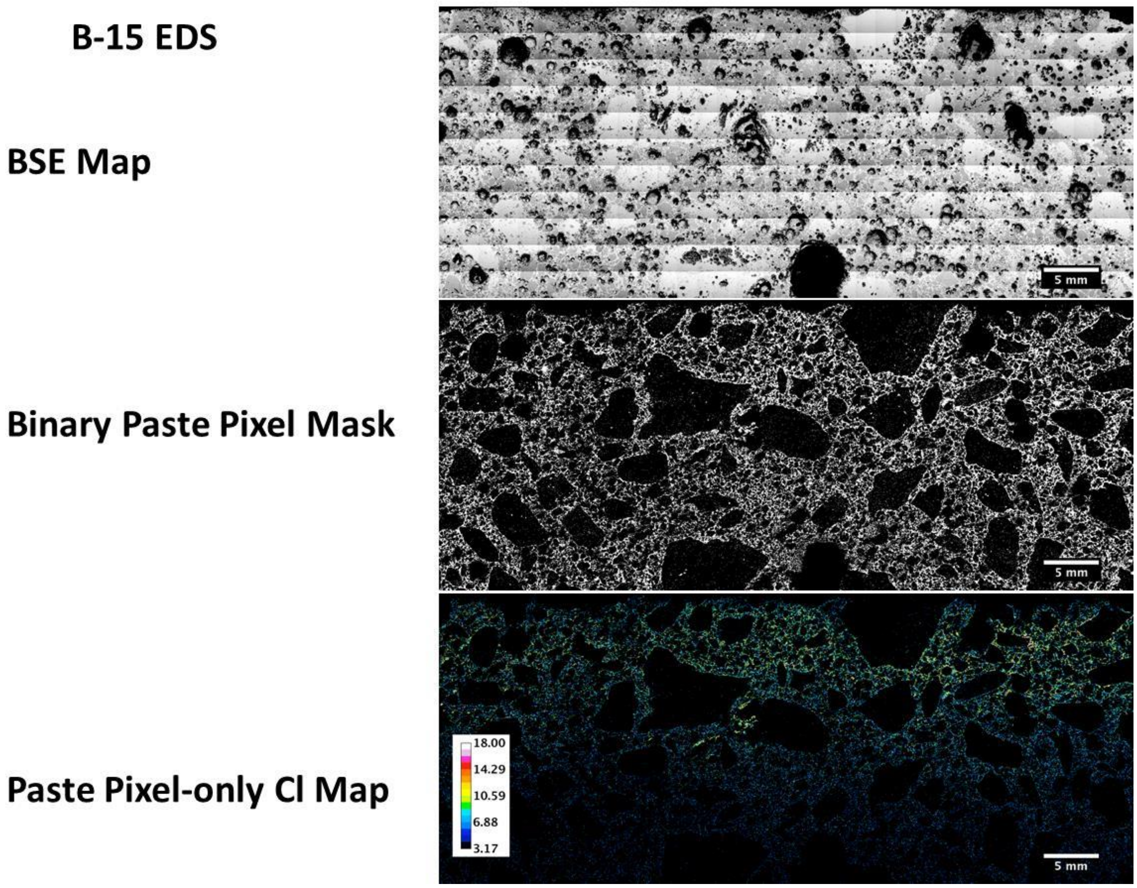

Figure 25 BSE imaging map, pixel mask, and Cl x-ray map corresponding to sample B-15 using SEM-EDS. Color code corresponds to Cl average counts

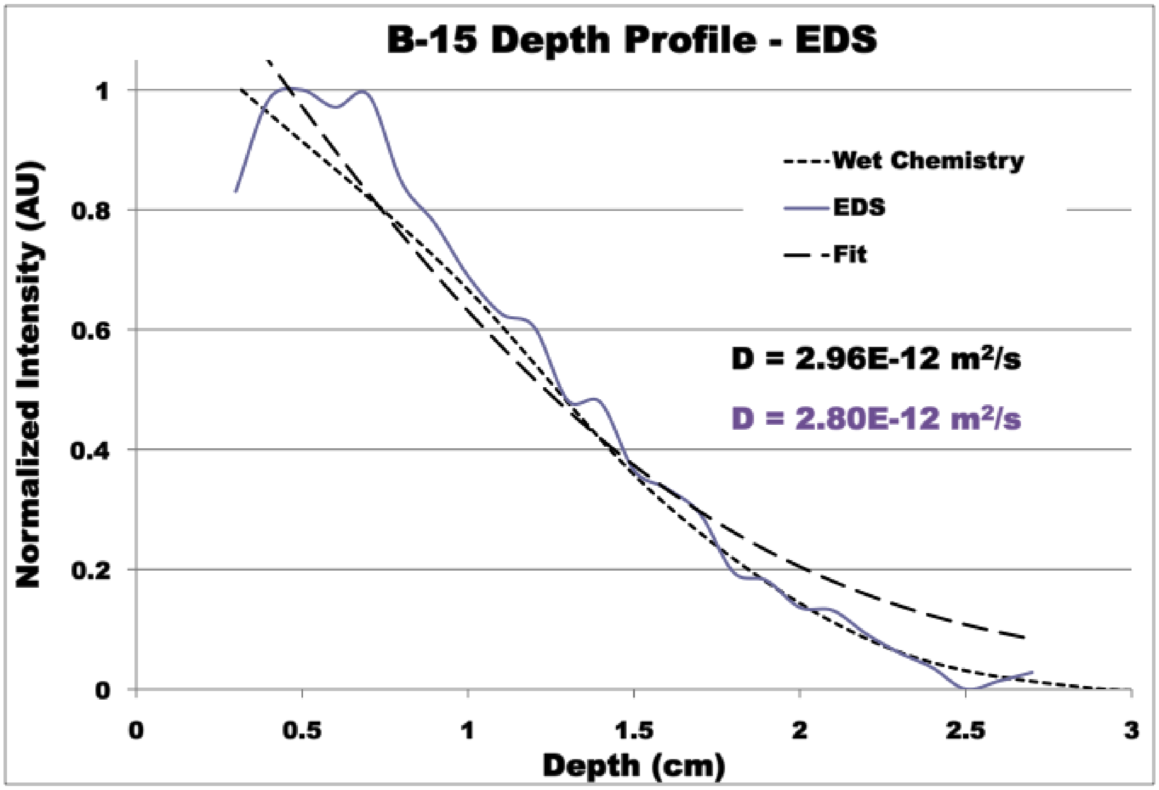

Figure 26 Normalized depth profile of sample B-15 with SEM-EDS

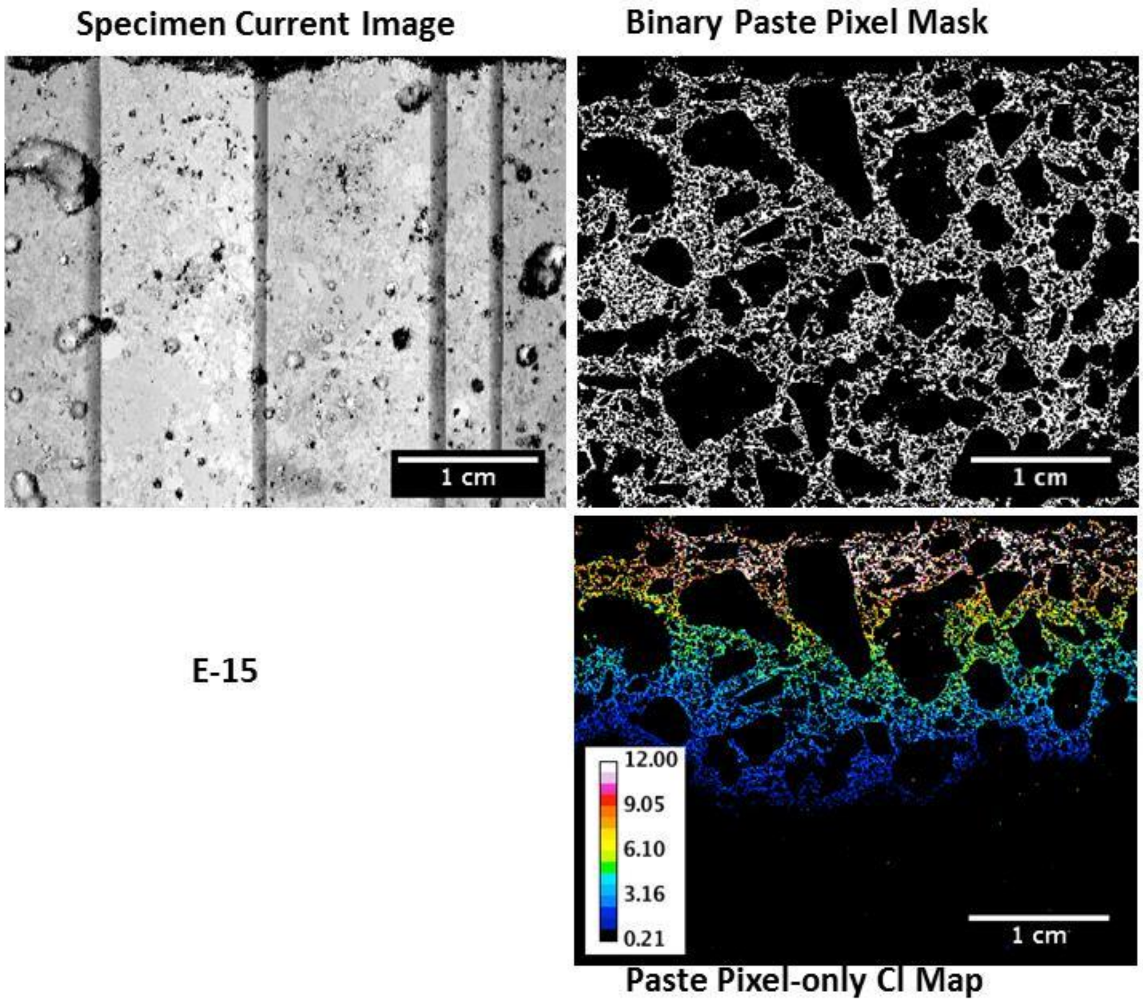

Figure 27 Specimen current image, pixel mask, and Cl x-ray map corresponding to sample E-15 using EPMA-WDS. Color code corresponds to Cl average count/s/nA

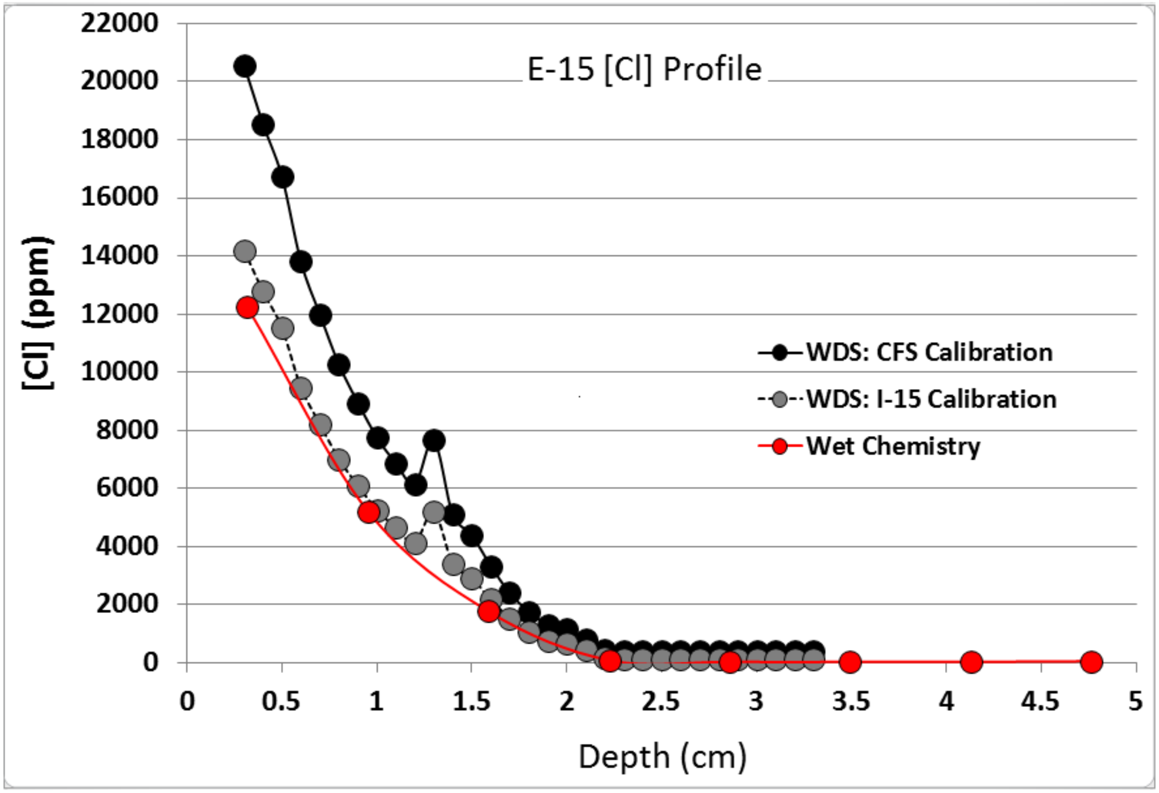

Figure 28 Concentration depth profile of sample E-15 with WDS

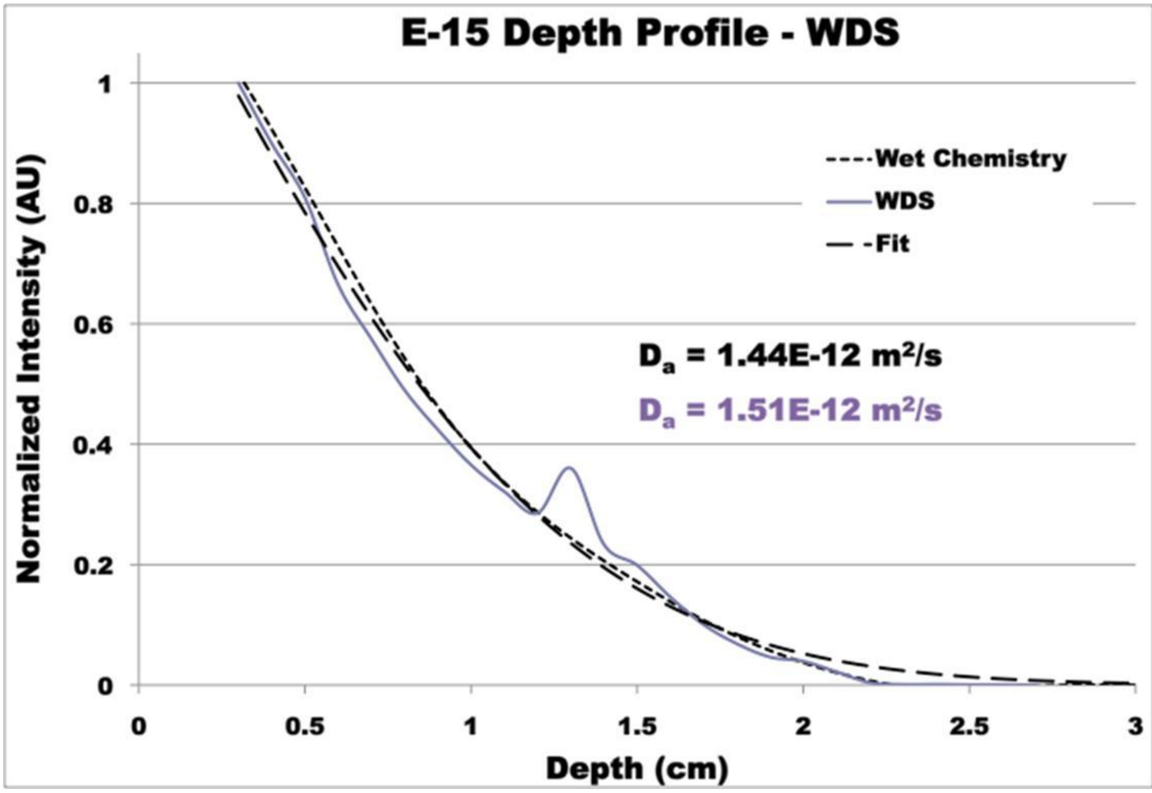

Figure 29 Normalized depth profile of sample E-15 with EPMA-WDS

E-15 EDS

BSE Map

Binary Paste Pixel Mask

Paste Pixel-only Cl Map

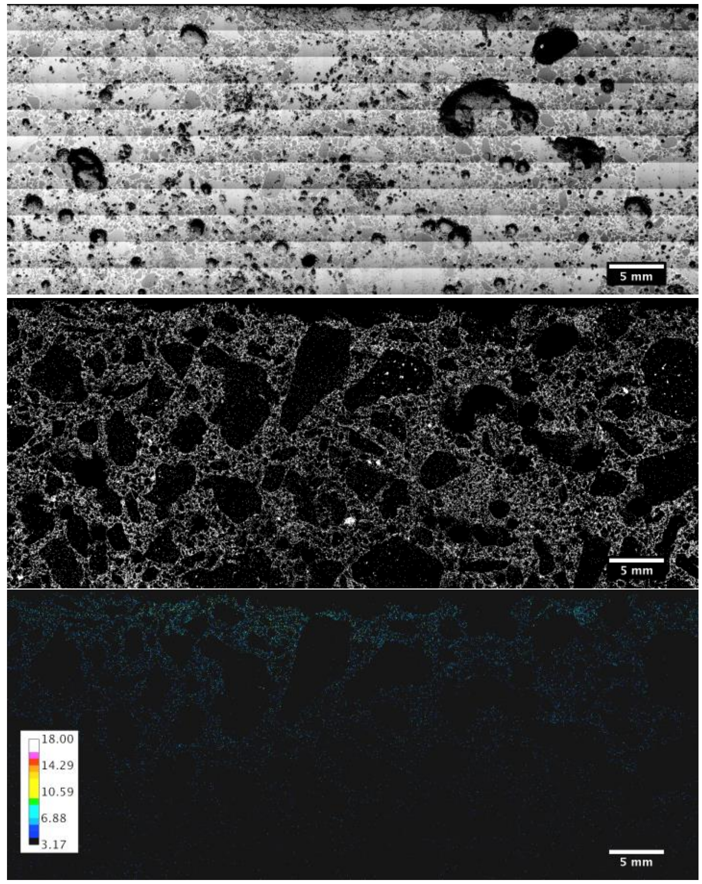

Figure 30 BSE imaging map, pixel mask, and Cl x-ray map corresponding to sample E-15 using SEM-EDS. Color code corresponds to Cl average counts

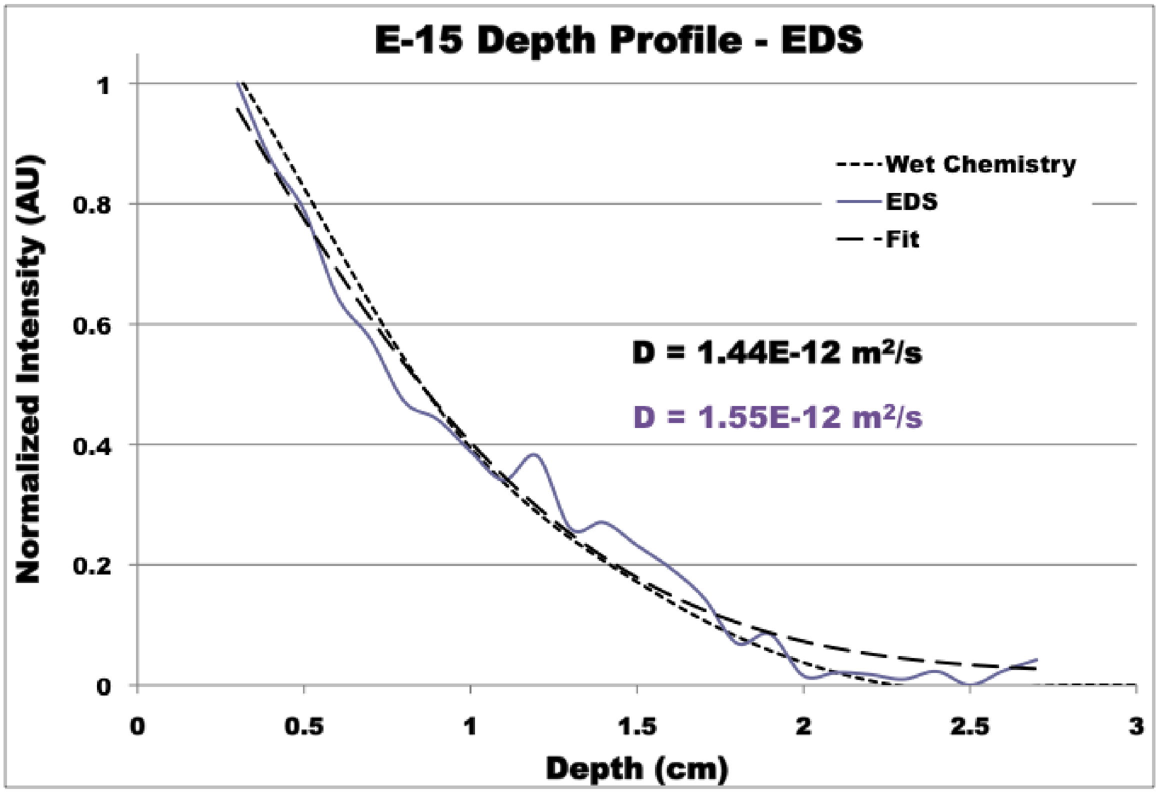

Figure 31 Normalized depth profile of sample B-15 with SEM-EDS

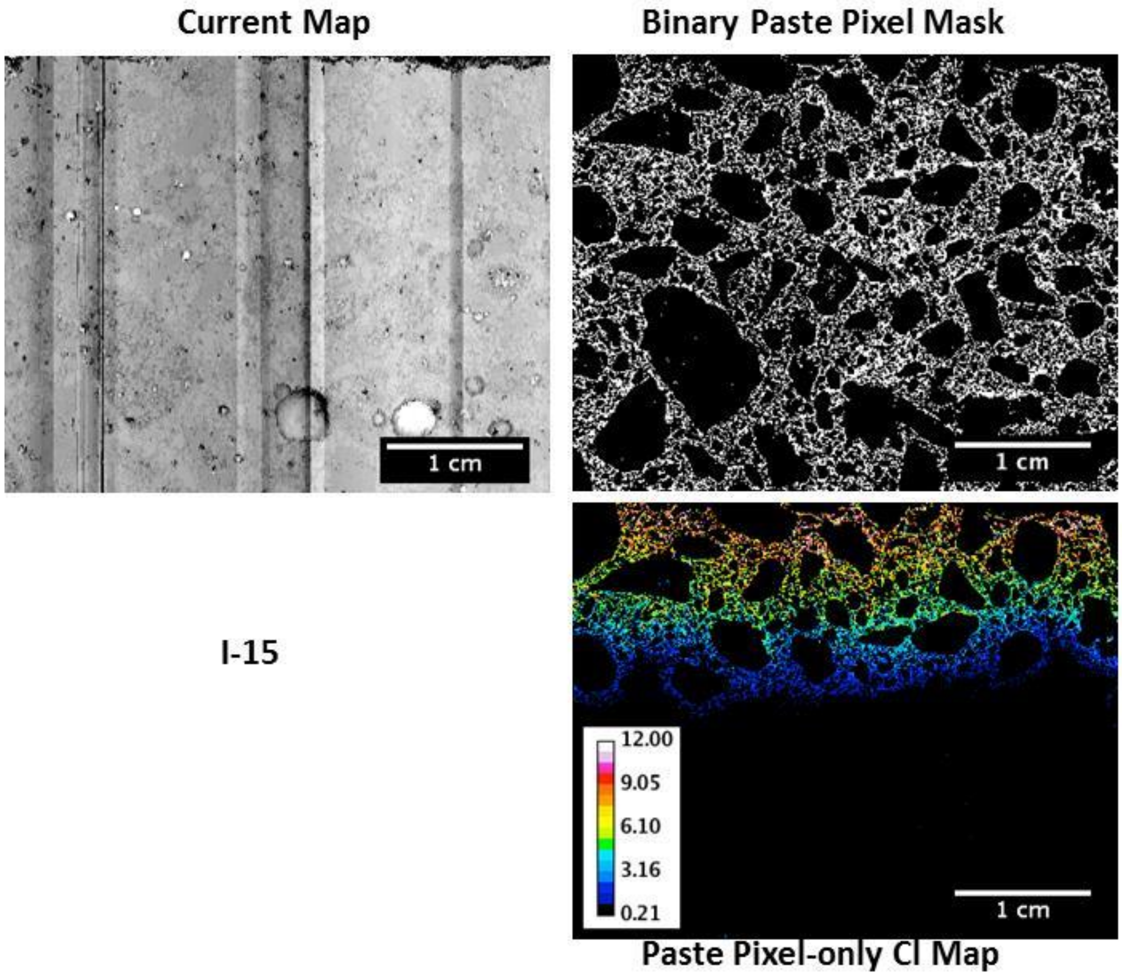

Figure 32 Specimen current image, pixel mask, and Cl x-ray map corresponding to sample I-15 using EPMA-WDS. Color code corresponds to Cl average count/s/nA

.

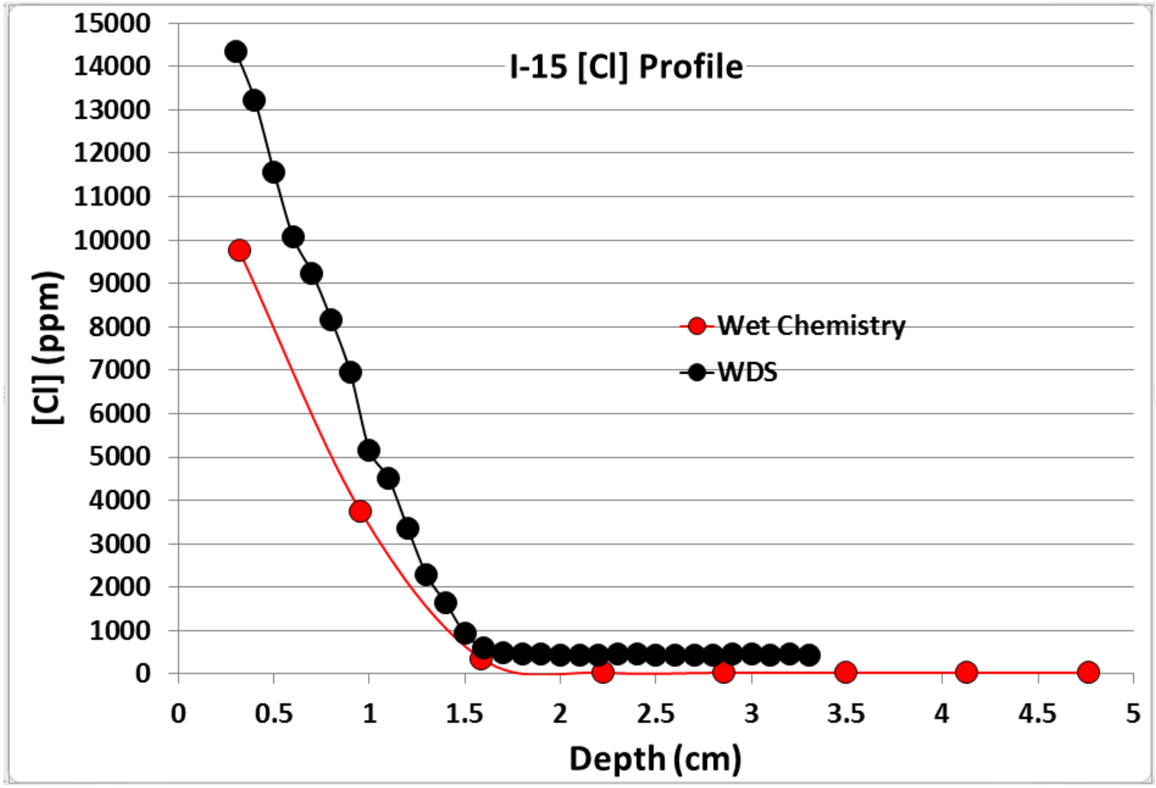

Figure 33 Concentration depth profile of sample I-15 with WDS

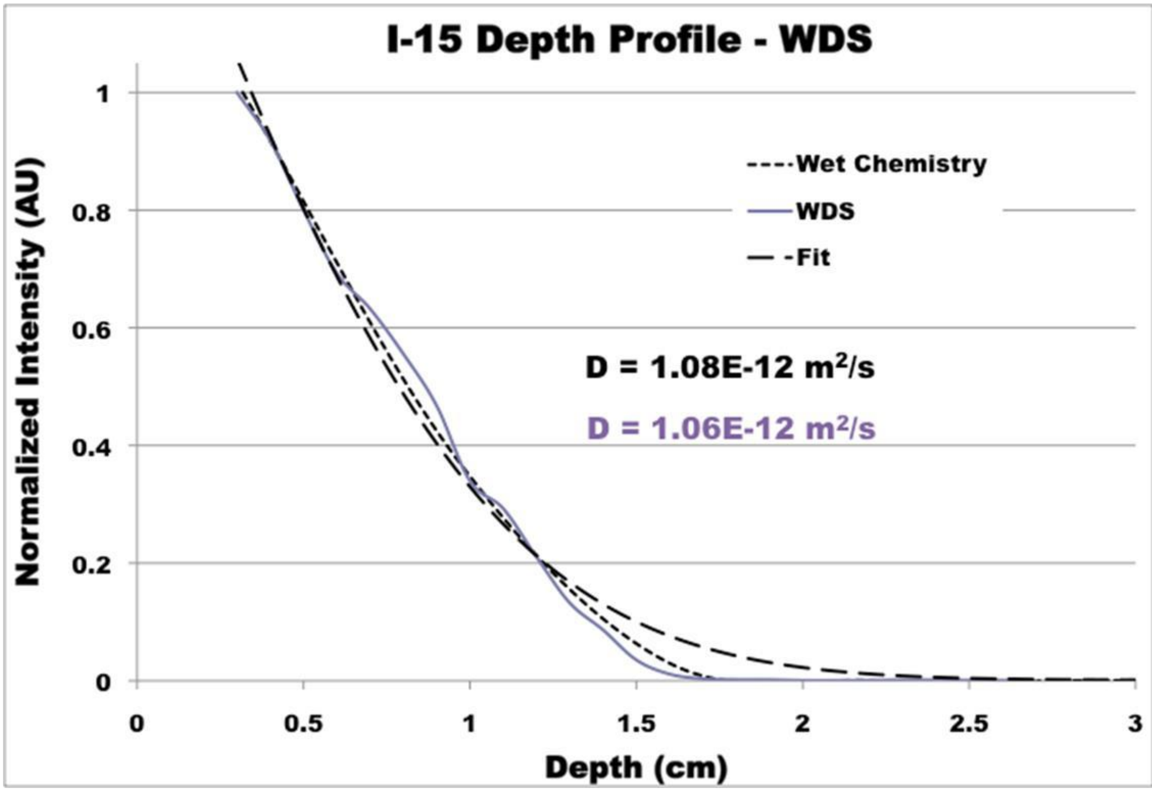

Figure 34 Normalized depth profile of sample I-15 with EPMA-WDS

I-15 EDS

BSE Map

Binary Paste Pixel Mask

Paste Pixel-only Cl Map

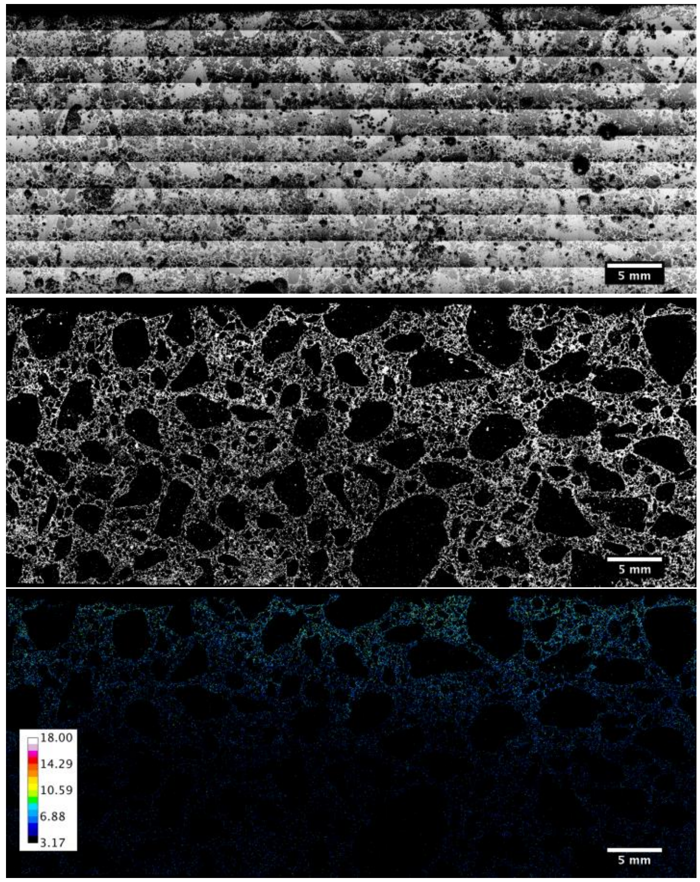

Figure 35 BSE imaging map, pixel mask, and Cl x-ray map corresponding to sample I-15 using SEM-EDS. Color code corresponds to Cl average counts

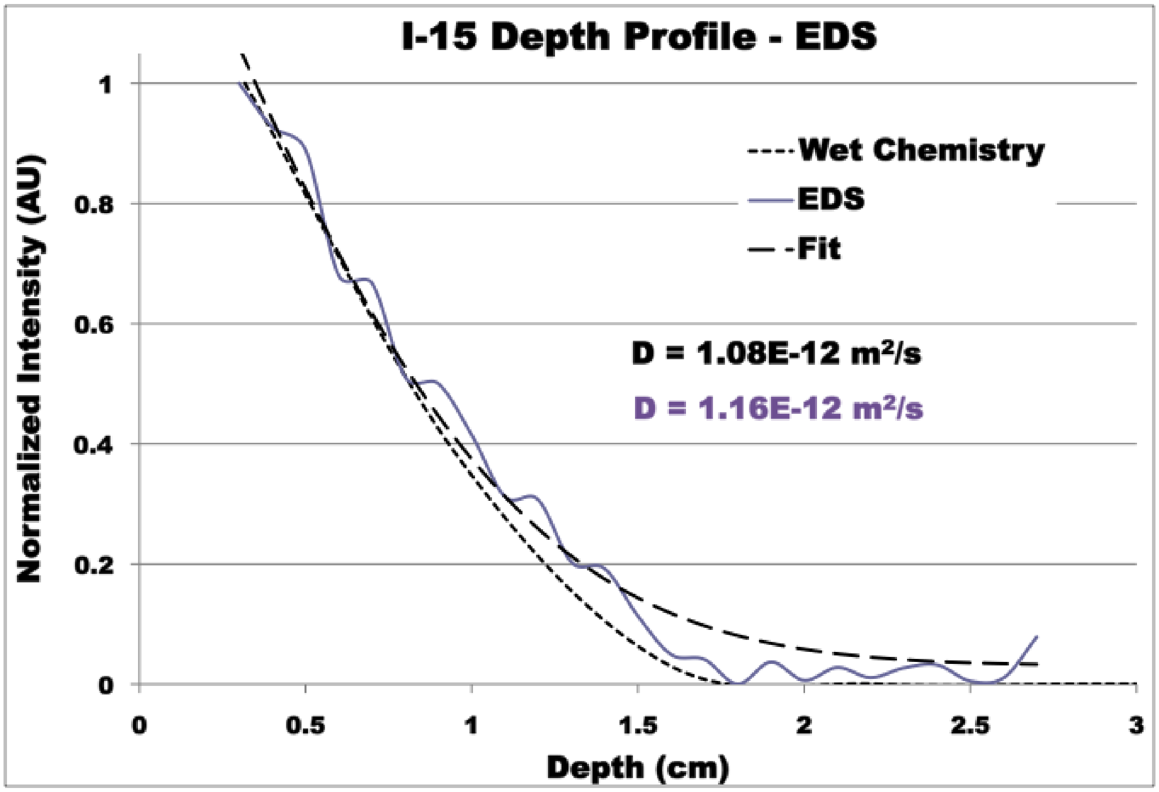

Figure 36 Normalized depth profile of sample I-15 with SEM-EDS

Method of Analysis

Let us examine the probe calibration data. The y-intercepts for the linear models (the counts per second per nano amperes (c/s/nA) that would be observed for a sample with 0 ppm Cl) are 0.231 and 0.214 c/s/nA for the 1-series and CFS series standards respectively. According to Mori et al., the limit of detection for probe method is defined as:

$$N_p - N_b > 3\sigma \qquad (1)$$

Where N_p is the count rate observed for the peak and N_b is the count rate measured of the background; σ is the standard deviation of $N_p - N_b$. The standard deviation of $N_p - N_b$ using the first samples in each series (no added Cl) is 0.006. Three times this value is 0.018 indicating that the limit of detection

(LOD) is < 0.005 wt. % Cl (5 ppm); this value is likely not a conservative enough estimate for the LOD. The average standard derivation for all the average N_p – N_b was 0.125, multiplied by three is ≈0.39 indicating and LOD of ≈300 ppm for our probe method. Given the fact that a simple t-test of the mean count rates obtained for standards 1 and 3 in both standard sets indicates that the count rates are significantly different (higher for 3 than 1) and the data presented above, we placed the LOD conservatively at the nominal LOD of 0.01 wt. % (100 ppm) for elements quantified using a microprobe.

The LOD for SEM-EDS is much higher than for EPMA (WDS). SEM-EDS offers a rapid mapping but not the sensitivity for the lower concentrations, while EPMA (WDS) offers a lower LOD. These techniques are complementary not substitutable. SEM-EDS has a 1000 ppm LOD, unlike EPMA (WDS) that can go as low as 100 ppm. In the case of cement and concrete samples the wet chemistry analysis is the proper method for evaluating absolute concentrations below 300 ppm.

Interestingly, Mori et al. define the variance of N_p – N_b as:

$$V = N_p + N_b \quad (2)$$

Applying the assumption that $N_p \approx N_b$ for elements present in trace concentrations yields:

$$V = 2N_b \ (3)$$

Hence the variance for 1 series and CFS series are 0.462 and 0.428, respectively, which yields a standard deviation of 0.68 and 0.65. Three times these amounts is ≈2 (≈3000 ppm) which is a tremendously over conservative estimate of the LOD of the probe method.

The simple criterion of three times the standard deviation of the background was applied to help estimate the LOD for the SEM-EDS x-ray mapping. This was done because maps of the background around the Cl peak could also be collected and analyzed on the standard samples at same time as all the other elements of interest. Results of the background study are summarized in Table 4.

If we take 0.72 as the average standard deviation of the background, three times this value would be 2.16; this value is however in conflict with the regression equation and reality as it yields a negative calculated Cl concentration. In fact, both regression equations yield negative values for the concentration of Cl for standard 1 and 3 in both sets. Both equations appear to generate non-negative values for standard 5 (≈500 ppm).

Applying the more stringent criterion that $N_p - N_b > 3\sigma$ sets the LOD for the SEM-EDS mapping method ≈ 0.1 – 0.2 wt. % (1000 – 2000 ppm), a nominal LOD for EDS detection. Both regression equations fit the data very well, evidenced by both coefficients of determination > 0.95, so an LOD of 1000 ppm for the method is a conservative estimate and the LOD could arguably be less than that to a lower limit of 500 ppm.

The average error estimated for the D_a values calculated with EDS data compared with the D_a values obtained through wet chemistry is 6.8%. The corresponding error for D_a values obtained with WDS data is 4.4%.

CHAPTER 5
DISCUSSION

Validity of hypothesis

An inspection of the weight percent concentration maps showed that the e-beam microanalysis methods used (SEM-EDS and EPMA-WDS) over-predicted the absolute concentration of Cl when compared with the values obtained by the wet chemistry method. However, when we normalized the data (microanalysis and wet chemistry), there is an excellent correspondence in the depth profile curves. The calculated D_a values from microanalysis data is on average within 7% error for EDS and 5% for WDS compared to the value given by the wet chemistry method.

It is important to note that the estimates of D_a look good, but the simple Fickian solution fit is ruled by the large value part of the profile, thus, the low concentration data could be removed and the same value could be obtained. If the goal is to look for potentially important benefits from chloride binding, the low concentration tail of the curve near the ~300 - 600 ppm threshold value – is critical. There is where the SEM method begins to lose accuracy while EPMA remains valuable.

Factors affecting the results

The close match of the curves after normalization indicated that there was a correction factor or offset that needed to be applied to the calibration equation that could then predict more accurately the wet chemistry values. Thus, we developed a method to estimate such correction factor using the data from the CFS series and found that it properly corrected the predicted concentration values to match quite closely the wet chemistry values.

We developed a calibration curve from I-15 and used it to quantify the other samples. This resulted in a much better match to the wet chemistry data which indicates that I-15 is a more suitable calibration standard than either of the standard series. Hence the choice of calibration standard can strongly impact the calculated absolute concentrations derived from X-ray maps.

An important point to explain is the e-beam time required for the analysis of the samples using EDS and WDS. The speed of collection and assembly of large scale images with BSE is critical to reduce the analysis time (x-ray intensity detection and processing). Once a BSE map is collected, regions of aggregate and paste can be clearly differentiated. Thus, an alternative to measure large scale areas is the collection of data along single linescans that go across paths that consist mainly of paste (as indicated in figure 26). These linescans perpendicular to the exposed surface can minimize the amount of data collected and the time required for quantitative analysis.

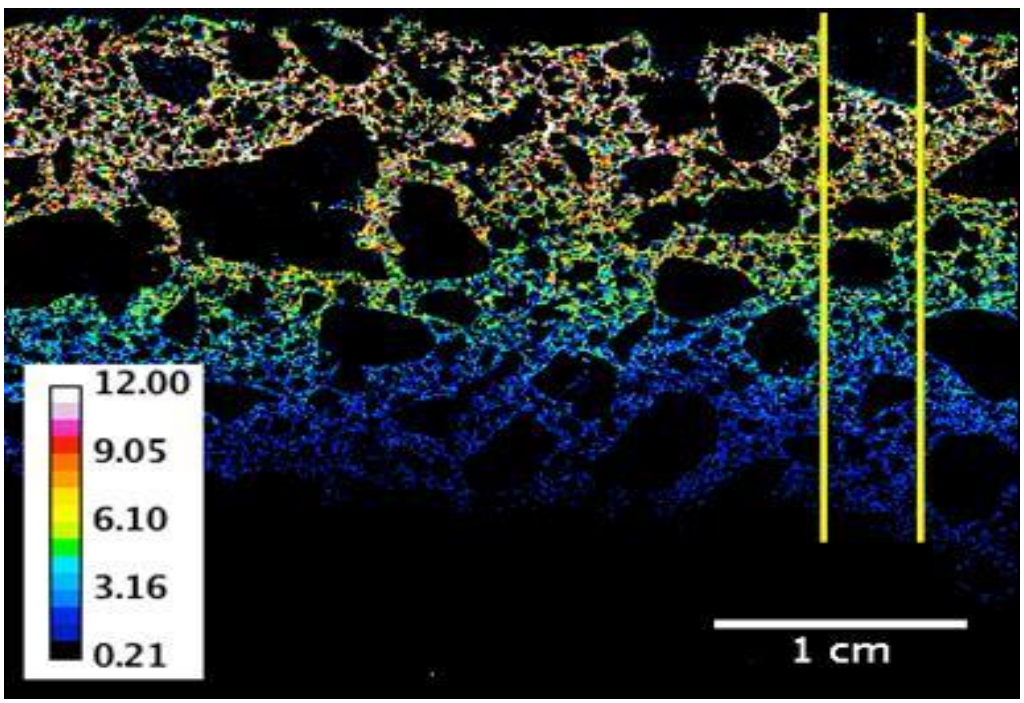

Figure 37 Proposed linescans across paste on sample B-15

Implications

The data and results strongly suggest that the e-beam X-ray mapping methods successfully adapted and developed by MAIC for both the SEM and EPMA instruments can be easily/readily used by FDOT-SMO to support and/or supplant currently employed methods for quantitative chloride profiling of concrete. These X-ray mapping methods provide a wealth of new information heretofore unavailable to FDOT-SMO that can now by applied to aid FDOT-SMO evaluation of concrete structure durability and remediation. Large-scale X-ray mapping could potentially help with the more efficient execution of FDOT-SMO's mission. While full maps might be cost prohibitive (8 h and $300 for wet chemistry analysis compared to 8 hours and $450 for SEM-EDS analysis), the benefits such as Chloride distribution maps, sample not getting destroyed, thousands of data points, and automated analysis, are clear. In any case the proposed less costly route of linescans should be further explored.

CHAPTER 6
CONCLUSIONS

Conclusions from the study

We sought to adapt and reproduce the methods and results described by Mori et al. above, and in a review [7], with the instrumentation available at MAIC for our work for FDOT-SMO. Additionally we developed a large scale x-ray mapping method with SEM instrumentation available at MAIC. At the present time, we know of no study like this for SEM. Thus, not only were we able to produce results mirroring to that of Mori et al. (on both instruments), but we also developed another paste-aggregate discrimination technique based on imaging as well as a standardless analysis method to determine Da based on normalized [Cl] data fit to Fick's 2nd diffusion law. Calculated D_a from data generated on both instruments agrees within 10% error to the calculated D_a values determined for the same samples by FDOT-SMO using the wet chemistry data/methodology.

We matched within a 7% or better error the diffusion coefficients calculated from wet chemistry data. In spite of the fact that the calibration curves over-predicted the concentration values, this did not impact the accuracy of the estimation of diffusion coefficients. Given that the estimation of diffusion coefficients was the end goal of the wet chemistry analysis, the presented methodology achieved the evaluation of the most sought parameter.

Standardless SEM-EDS estimation of diffusion coefficients was the most expeditious method of sample analysis. If the interest was focused on the estimation of absolute concentrations, corrected calibration curves using standards and EPMA were the most appropriate route.

Summary of Conclusions

MAIC has successfully adapted and developed an automated e-beam X-ray mapping method for cementitious samples using both the SEM and EPMA. This X-ray mapping method can provide quantitative microscopic images of chlorine distribution over a large area of a sample using as well as distribution data for other elements simultaneously. The D_a for chloride diffusion in concrete samples can potentially be determined more rapidly with X-ray mapping while preserving samples for future analysis and minimizing hazardous waste generation. This study is a strong independent confirmation of the utility and applicability of e-beam X-ray mapping for organizations such as FDOT-SMO to use in the monitor, study, repair and improvement of cement and concrete materials and structures.

Recommendations

A new instrument with a configuration tailored to the needs of this methodology is recommended. A standard system comes with an x-ray detector for EDS and four WDS spectrometers at a price on the $1M range. However, EDS and only two spectrometers are necessary with one crystal each (for Cl and S) if the system will be a dedicated system to perform the analysis of Cl. This gets the price of a new system significantly lower. A used system, with a few years of use, is also a good alternative and reduces even further the cost of the instrument.

Sample preparation is fundamental in the generation of good data. The FDOT-SMO and the MAIC do not have in-house the capabilities to do a sample preparation comparable to that done by APS. Thus, it is recommended to either develop in-house the sample preparation method or negotiate a high volume/ long term arrangement with APS so sample preparation costs are minimized.

References

[1] Goldstein, J.I., Newbury, D.E., Echlin. P., Joy, D.C., Romig, A.D. Jr., Lyman, C.E., Fiori, C., and Lifshin, E. *Scanning Electron Microscopy and X-Ray Microanalysis, A Text for Biologists, Materials Scientists, and Geologists*. Kluwer Academic/Plenum Publishers, 2003.

[2] RBD Instruments, http://www.rbdinstruments.com/Products/Refurbished ItemsInfo/660Info/sample%20interaction.jpg (accessed March 13, 2013).

[3] Intech Open Access Publisher, http://www.intechopen.com/source /html/30937/media/image3.png (accessed March 13, 2013).

[4] Belgian Nuclear Research Center, http://www.sckcen.be/microstructure/ Infrastructure/SEM/Infrastructure_SEM_Jeol6310.htm (accessed March 13, 2013)

[5] Jensen, O.M., Coats, A.M., and Glasser, F.P. "Chloride ingress profiles measured by electron probe micro-analysis." *Cement and Concrete Research* 26, no. 11 (1996).

[6] Mori, D., Yamada, K., Hosokawa, Y., and Yamamoto M. "Applications of Electron Probe Microanalyzer for Measurement of Cl Concentration Profile in Concrete." *Journal of Advanced Concrete Technology* 4, no. 3 (2006).

[7] Mori, D. and Yamada, K. "A review of Recent Applications of EPMA to Evaluate the Durability of Concrete." *Journal of Advanced Concrete Technology* 5, no. 3 (2007).

Appendix

1) Summary of data:

Table's columns headings:

Bkg Mean: Calculated average background (not characteristic) x-ray counts generated from all pixel collection areas

Bkg StdDev: Standard deviation of the background mean

[Cl] (ppm) CFS Cal/[Cl] (ppm) I-15 Cal: Calculated chlorine concentration using either the calibration equation derived for the CFS standard series of from the I-15 sample gradient

EPMA Cts Std Dev (Raw Data): Standard deviation of the mean counts

EPMA Cts Std Err of Mean: Standard deviation of the mean counts divided by the number of collection points/pixels

Depth: For chloride determination, the sample is cut into slices parallel to the chloride-exposed surface (physical slices for wet chemical analysis, virtual for e-beam analysis). For the wet chemical analysis, the thickness of each slice was ~6.35mm, 1/4" (Except for the first slice). The listed value is the depth into the sample of the bottom of each successive slice.

Depth (Tables 9,11,13,15,17,19): Distance into the sample normal to the chloride-exposed surface.

FDOT Wet Chem (ppm): results of wet chemistry analysis measured in ppm

FDOT Wet Chem (wt%): results of wet chemistry analysis measured in weight percent

Mean Cts – EPMA: Average of all characteristic Cl x-ray counts divided by the count time (dwell time) and the measured specimen current for each collected point/pixel (counts/s/nA)

Mean: Calculated average characteristic Cl x-ray counts from all collected pixels

Normalized Intensity (AU) (Tables 8,10,12,14,16,18): A min-max normalization of the raw ppm data to simplify input to the curve fitting program while preserving the relation of data points to one another. The resulting values fall in the computationally convenient range [0,1]

$$I_{x_{norm}} = \frac{I_x - Min(I)}{Max(I) - Min(I)} = \frac{I_x - Min(I)}{Range(I)}$$

Where I is the entire set of raw intensity values and I_x is the intensity value (in arbitrary units, AU) corresponding to a particular depth

Normalized Intensity (AU) (Tables 9,11,13,15,17,19): Normalized intensity for chlorine concentration calculated using curve fitting

SEM Cts StdDev (Raw Data): Standard deviation of the mean counts

SEM Cts StdErr of Mean: Standard deviation of the mean counts divided by the number of collection points/pixels

StdDev: Standard deviation of the mean

Wet Chemistry (ppm): Chloride concentration in ppm determined by the FDOT-SMO wet chemical method for each successive slice

WDS (Cts/s/nA): The calculated average from all paste pixels in the nearest 1mm virtual slice thickness (generated from the image processing) of the characteristic Cl characteristic x-ray counts divided by dwell time and specimen current

Raw ppm: Chloride concentration in ppm determined by the FDOT-SMO wet chemical method for each successive slice

Raw counts: The calculated average from all paste pixels in the 1mm virtual slice thickness (generated from the image processing) of the characteristic Cl characteristic x-ray WDS counts divided by dwell time and specimen current (counts/s/nA)

<u>Tabulated Data:</u>

Table 2: Data corresponding to the mixes of the series 1 of cement-chloride standards

Series 1 Chloride Standards (w/c = 0.35)							
Series 1 (Mix)	Mix	Cl^- Design	Cl^- ppm added	Weight Cl^- (g)	Weight NaCl (g)	Cement Weight (g)	Water Weight (g)
1-1	Control	Background (Bg)	0	0.0000	0.0000	296.296	103.704
1-2	50 ppm	Bg + 50 ppm	50	0.0200	0.0330	296.272	103.695
1-3	100 ppm	Bg + 100 ppm	100	0.0400	0.0659	296.247	103.687
1-4	200 ppm	Bg + 200 ppm	200	0.0800	0.1319	296.199	103.670
1-5	400 ppm	Bg + 400 ppm	400	0.1600	0.2638	296.101	103.635
1-6	600 ppm	Bg + 600 ppm	600	0.2400	0.3956	296.003	103.601
1-7	800 ppm	Bg + 800 ppm	800	0.3200	0.5275	295.906	103.567
1-8	1000ppm	Bg + 1000ppm	1000	0.4000	0.6594	295.808	103.533
1-9	2000ppm	Bg + 2000ppm	2000	0.8000	1.3188	295.319	103.362
1-10	4000ppm	Bg + 4000ppm	4000	1.6000	2.6377	294.342	103.020
1-11	6000ppm	Bg + 6000ppm	6000	2.4000	3.9565	293.366	102.678
1-12	8000ppm	Bg + 8000ppm	8000	3.2000	5.2753	292.389	102.336
1-13	10000ppm	Bg + 10000ppm	10000	4.0000	6.5941	291.412	101.994

Table 3 Data corresponding to the mixes of the CFS series of cement-chloride standards

CFS Series Chloride Standards (w/c = 0.35)									
CFS (Mix)	Mix (ppm)	Cl^- Design	Cl^- ppm added	Cl^- (g)	NaCl (g)	Cement (g)	FlyAsh (g)	Sand (g)	Water (g)
1	Control	Background (Bg)	0	0.0000	0.0000	354.610	70.922	424.681	149.787
2	50	Bg + 50 ppm	50	0.0500	0.0824	354.581	70.916	424.646	149.775
3	100	Bg + 100 ppm	100	0.1000	0.1649	354.551	70.910	424.611	149.763
4	200	Bg + 200 ppm	200	0.2000	0.3297	354.493	70.899	424.541	149.738
5	400	Bg + 400 ppm	400	0.4000	0.6594	354.376	70.875	424.401	149.688
6	600	Bg + 600 ppm	600	0.6000	0.9891	354.259	70.852	424.261	149.639
7	800	Bg + 800 ppm	800	0.8000	1.3188	354.142	70.828	424.121	149.590
8	1000	Bg + 1000ppm	1000	1.0000	1.6485	354.025	70.805	423.981	149.540
9	2000	Bg + 2000ppm	2000	2.0000	3.2971	353.441	70.688	423.281	149.293
10	4000	Bg + 4000ppm	4000	4.0000	6.5941	352.272	70.454	421.880	148.800
11	6000	Bg + 6000ppm	6000	6.0000	9.8912	351.102	70.220	420.480	148.306
12	8000	Bg + 8000ppm	8000	8.0000	13.1883	349.933	69.987	419.080	147.812
13	10000	Bg + 10000ppm	10000	10.0000	16.4853	348.764	69.753	417.680	147.318

Table 4 EPMA/WDS calibration curves raw data for the 1-series and CFS standards

1 Series					
Std	FDOT Wet Chem (ppm)	FDOT Wet Chem (wt %)	Mean Cts - EPMA	EPMA Cts StdDev (Raw Data)	EPMA Cts StdErr of Mean
1	159.2	0.01592	0.25852	0.09426	0.002061344
3	227.6	0.02276	0.33322	0.13235	0.002894323
5	506.6	0.05066	0.42815	0.1309	0.002862613
7	984.7	0.09847	0.59624	0.14535	0.003178616
9	2216.2	0.22162	1.18516	0.36642	0.008013129
11	6495.6	0.64956	2.78901	0.4285	0.009370738
13	10763.6	1.07636			

CFS Series					
Std	FDOT Wet Chem (ppm)	FDOT Wet Chem (wt %)	Mean Cts - EPMA	EPMA Cts StdDev (Raw Data)	EPMA Cts StdErr of Mean
1	113.6	0.01136	0.233	0.0881	0.001926633
3	211.8	0.02118	0.303	0.0998	0.002182496
5					
7	1036.3	0.10363	0.774	0.208	0.00454869
9	2204.3	0.22043	1.66	0.4086	0.008935551
11	6201	0.6201			
13	9869.4	0.98694	5.95	1.2413	0.027145618

Table 5 SEM-EDS calibration curves raw data for the 1-series and CFS standards

1 Series					
Std	FDOT Wet Chem (ppm	FDOT Wet Chem (wt %)	Mean Cts - SEM	SEM Cts StdDev (Raw Data)	SEM Cts StdErr of Mean
1	159.2	0.01592	2.81101	1.68879	0.036931643
3	227.6	0.02276	3.24233	1.81762	0.039748988
5	506.6	0.05066	3.32699	1.84222	0.040286958
7	984.7	0.09847	3.43989	1.8506	0.040470218
9	2216.2	0.22162	3.74888	1.97924	0.043283407
11	6495.6	0.64956	4.48906	2.22819	0.048727621
13	10763.6	1.07636	5.15744	2.49022	0.054457876

CFS Series					
Std	FDOT Wet Chem (ppm	FDOT Wet Chem (wt %)	Mean Cts - SEM	SEM Cts StdDev (Raw Data)	SEM Cts StdErr of Mean
1	113.6	0.01136	3.052	1.7809	0.038945969
3	211.8	0.02118	3.122	1.7893	0.039129666
5					
7	1036.3	0.10363	3.397	1.8618	0.040715147
9	2204.3	0.22043	3.877	2.1296	0.046571585
11	6201	0.6201	4.648	2.5072	0.054829207
13	9869.4	0.98694	5.145	2.7721	0.060622226

Table 6 Results of the background analysis of SEM-EDS data

1 Series					
Standard	Mean	StdDev	Bkg Mean	Bkg StdDev	Wet Chem ppm
1	2.811	1.6888	0.4596	0.6794	159.2
3	3.2423	1.8176	0.5236	0.7238	227.6
5	3.327	1.8422	0.5302	0.7273	506.6
7	3.4399	1.8506	0.535	0.7261	984.7
9	3.7489	1.9792	0.5456	0.739	2216.2
11	4.4891	2.2282	0.5551	0.7406	6495.6
13	5.1574	2.4902	0.5573	0.7464	10763.6
			0.5294857	0.726085714	
CFS Series					
Standard	Mean	StdDev	Bkg Mean	Bkg StdDev	Wet Chem ppm
1	3.0522	1.7809	0.4804	0.6957	113.6
3	3.1223	1.7893	0.4806	0.6961	211.8
7	3.2688	1.8618	0.4917	0.7001	1036.3
9	3.8767	2.1296	0.5128	0.7198	2204.3
11	4.6481	2.5072	0.506	0.7143	6201
13	5.1449	2.7721	0.503	0.7105	9869.4
			0.49575	0.706083333	

Table 7 Data corresponding to the wet chemistry and WDS analysis for sample B-15 calibration curve

Derived Calibration B-15		
Depth (cm)	Wet Chemistry (ppm)	WDS (Cts/s/nA)
0.3175	9561.754386	8.075
0.9525	6639.649123	5.493
1.5875	3017.631579	2.805
2.2225	792.6315789	0.966
2.8575	68.94736842	0.249

Table 8 Data corresponding to the wet chemistry and WDS analysis for sample E-15 calibration curve

Derived Calibration E-15		
Depth (cm)	**Wet Chemistry (ppm)**	**WDS (Cts/s/nA)**
0.3175	12243.50877	12.016
0.9525	5224.736842	4.535
1.5875	1774.824561	1.946
2.2225	92.36842105	0.27
2.8575	35.61403509	0.227

Table 9 Data corresponding to the wet chemistry and WDS analysis for sample I-15 calibration curve

Derived Calibration I-15		
Depth (cm)	**Wet Chemistry (ppm)**	**WDS (Cts/s/nA)**
0.3175	9765.964912	8.386
0.9525	3760.789474	3.018
1.5875	355.5263158	0.348
2.2225	31.49122807	0.261
2.8575	32.80701754	0.267

Table 10 Raw and normalized data corresponding to the wet chemistry analysis and the WDS analysis of sample B-15 for concentration depth profile

B-15 Depth Profile - WDS							
Wet Chemistry			WDS				
Depth (cm)	Raw ppm	Normalized Intensity (AU)	Depth (cm)	Raw counts	[Cl] (ppm) CFS Cal	[Cl] (ppm) I-15 Cal	Normalized Intensity (AU)
0.3175	9561.7544	1	0.1	5.321	9111.08737	6209.4798	
0.9525	6639.6491	0.69314382	0.2	7.723	13224.10107	9076.9874	
1.5875	3017.6316	0.312788438	0.3	8.075	13826.84079	9497.205	0.926030624
2.2225	792.63158	0.079136691	0.4	8.116	13897.04627	9546.1508	0.930859835
2.8575	68.947368	3.14E-03	0.5	8.483	14525.47093	9984.2754	0.974087161
3.4925	39.035088	0	0.6	8.307	14224.10107	9774.1666	0.95335689
4.1275	41.052632	2.12E-04	0.7	8.703	14902.18326	10246.9114	1
4.7625	40.438596	0.000147385	0.8	6.066	10386.7723	7098.8608	0.689399293
			0.9	6.079	10409.03258	7114.3802	0.690930506
			1	5.493	9405.607918	6414.8134	0.621908127
			1.1	5.269	9022.046274	6147.4022	0.595524146
			1.2	5.037	8624.786	5870.4406	0.56819788
			1.3	4.548	7787.457233	5286.6724	0.510600707
			1.4	4.084	6992.936685	4732.7492	0.455948174
			1.5	3.33	5701.840795	3832.624	0.367137809
			1.6	2.805	4802.868192	3205.879	0.305300353
			1.7	2.384	4081.977781	2703.2892	0.255712603
			1.8	2.063	3532.320247	2320.0794	0.217903416
			1.9	1.776	3040.88189	1977.4588	0.18409894
			2	1.443	2470.676411	1579.9234	0.144876325
			2.1	1.194	2044.306548	1282.6672	0.115547703
			2.2	0.966	1653.895589	1010.4808	0.08869258
			2.3	0.759	1299.443534	763.3642	0.064310954
			2.4	0.514	879.9229863	470.8832	0.035453475
			2.5	0.394	674.4435342	327.6272	0.021319199
			2.6	0.325	556.2928493	245.255	0.013191991
			2.7	0.282	482.6627123	193.9216	0.008127208
			2.8	0.287	491.2243562	199.8906	0.008716137
			2.9	0.249	426.155863	154.5262	0.004240283
			3	0.236	403.895589	139.0068	0.002709069
			3.1	0.237	405.6079178	140.2006	0.002826855
			3.2	0.453	775.4709315	398.0614	0.028268551
			3.3	0.213	364.5120274	111.5494	0

Table 11 Data corresponding to the normalized WDS intensities used for the depth profile fit curve for sample B-15

Fit							
Depth (cm)	Normalized Intensity (AU)	Depth (cm)	Normalized Intensity (AU)	Depth (cm)	Normalized Intensity (AU)	Depth (cm)	Normalized Intensity (AU)
0.3	1.103208857	1.008543	0.602832092	1.7623116	0.251653179	2.5160804	0.083933222
0.3150754	1.091392315	1.023618	0.593793247	1.7773869	0.246692643	2.5311558	0.081965628
0.3301508	1.079607805	1.038693	0.58483376	1.7924623	0.241807485	2.5462312	0.080040475
0.3452261	1.067856765	1.053769	0.575954087	1.8075377	0.236997184	2.5613065	0.078157092
0.3603015	1.056140622	1.068844	0.567154662	1.8226131	0.232261209	2.5763819	0.076314812
0.3753769	1.044460789	1.08392	0.558435889	1.8376884	0.227599016	2.5914573	0.074512972
0.3904523	1.032818667	1.098995	0.549798154	1.8527638	0.223010052	2.6065327	0.072750912
0.4055276	1.021215639	1.11407	0.541241813	1.8678392	0.218493753	2.621608	0.071027979
0.420603	1.009653078	1.129146	0.5327672	1.8829146	0.214049546	2.6366834	0.069343522
0.4356784	0.998132337	1.144221	0.524374624	1.8979899	0.209676848	2.6517588	0.067696897
0.4507538	0.986654756	1.159296	0.516064372	1.9130653	0.205375067	2.6668342	0.066087462
0.4658291	0.97522166	1.174372	0.507836703	1.9281407	0.201143603	2.6819095	0.064514582
0.4809045	0.963834353	1.189447	0.499691856	1.9432161	0.196981847	2.6969849	0.062977625
0.4959799	0.952494127	1.204523	0.491630043	1.9582915	0.192889182	2.7120603	0.061475968
0.5110553	0.941202252	1.219598	0.483651455	1.9733668	0.188864983	2.7271357	0.060008989
0.5261307	0.929959983	1.234673	0.475756257	1.9884422	0.18490862	2.7422111	0.058576074
0.541206	0.918768555	1.249749	0.467944593	2.0035176	0.181019453	2.7572864	0.057176613
0.5562814	0.907629186	1.264824	0.460216582	2.018593	0.177196839	2.7723618	0.055810004
0.5713568	0.896543072	1.279899	0.452572322	2.0336683	0.173440125	2.7874372	0.054475647
0.5864322	0.885511393	1.294975	0.445011886	2.0487437	0.169748656	2.8025126	0.053172952
0.6015075	0.874535306	1.31005	0.437535328	2.0638191	0.166121769	2.8175879	0.051901332
0.6165829	0.863615951	1.325126	0.430142676	2.0788945	0.162558797	2.8326633	0.050660206
0.6316583	0.852754443	1.340201	0.422833938	2.0939698	0.159059069	2.8477387	0.049449002
0.6467337	0.84195188	1.355276	0.4156091	2.1090452	0.155621908	2.8628141	0.048267151
0.661809	0.831209337	1.370352	0.408468126	2.1241206	0.152246634	2.8778894	0.047114092
0.6768844	0.820527868	1.385427	0.401410959	2.139196	0.148932564	2.8929648	0.045989268
0.6919598	0.809908505	1.400503	0.394437523	2.1542714	0.145679009	2.9080402	0.044892132
0.7070352	0.799352258	1.415578	0.387547717	2.1693467	0.142485281	2.9231156	0.043822141
0.7221106	0.788860115	1.430653	0.380741423	2.1844221	0.139350685	2.938191	0.042778759
0.7371859	0.77843304	1.445729	0.374018502	2.1994975	0.136274527	2.9532663	0.041761455
0.7522613	0.768071976	1.460804	0.367378795	2.2145729	0.133256108	2.9683417	0.040769708
0.7673367	0.757777842	1.475879	0.360822124	2.2296482	0.130294731	2.9834171	0.039803
0.7824121	0.747551534	1.490955	0.354348291	2.2447236	0.127389694	2.9984925	0.038860822
0.7974874	0.737393924	1.50603	0.34795708	2.259799	0.124540296	3.0135678	0.037942671
0.8125628	0.727305861	1.521106	0.341648255	2.2748744	0.121745834	3.0286432	0.03704805
0.8276382	0.71728817	1.536181	0.335421564	2.2899497	0.119005604	3.0437186	0.036176469
0.8427136	0.707341652	1.551256	0.329276734	2.3050251	0.116318904	3.058794	0.035327445
0.8577889	0.697467084	1.566332	0.323213478	2.3201005	0.113685029	3.0738693	0.034500502
0.8728643	0.687665218	1.581407	0.31723149	2.3351759	0.111103276	3.0889447	0.03369517
0.8879397	0.677936782	1.596482	0.311330446	2.3502513	0.108572942	3.1040201	0.032910986
0.9030151	0.668282482	1.611558	0.305510008	2.3653266	0.106093326	3.1190955	0.032147495
0.9180905	0.658702995	1.626633	0.299769819	2.380402	0.103663727	3.1341709	0.031404245
0.9331658	0.649198976	1.641709	0.294109509	2.3954774	0.101283444	3.1492462	0.030680796
0.9482412	0.639771056	1.656784	0.28852869	2.4105528	0.098951779	3.1643216	0.029976711
0.9633166	0.630419839	1.671859	0.283026962	2.4256281	0.096668036	3.179397	0.02929156
0.978392	0.621145907	1.686935	0.277603908	2.4407035	0.094431521	3.1944724	0.02862492
0.9934673	0.611949814	1.70201	0.272259096	2.4557789	0.092241542	3.2095477	0.027976377
		1.717085	0.266992082	2.4708543	0.090097407	3.2246231	0.027345521
		1.732161	0.261802408	2.4859296	0.087998432	3.2396985	0.026731948
		1.747236	0.256689601	2.501005	0.08594393	3.2547739	0.026135264
						3.2698492	0.025555078
						3.2849246	0.024991007
						3.3	0.024442676

Table 12 Raw and normalized data corresponding to the wet chemistry analysis and the WDS analysis of sample E-15 for concentration depth profile

E-15 Depth Profile - WDS							
Wet Chemistry			WDS				
Depth (cm)	Raw ppm	Normalized Intensity (AU)	Depth (cm)	Raw Counts	[Cl] (ppm) CFS Cal	[Cl] (ppm) i-15 Cal	Normalized Intensity (AU)
0.3175	12243.50877	1	0.1	9.915	16977.52573	11693.797	
0.9525	5224.736842	0.425082451	0.2	12.119	20751.49833	14324.9322	
1.5875	1774.824561	0.142484534	0.3	12.016	20575.12847	14201.9708	1
2.2225	92.36842105	0.004677631	0.4	10.831	18546.01888	12787.3178	0.899516662
2.8575	35.61403509	2.16E-05	0.5	9.77	16729.23805	11520.696	0.809548037
3.4925	35.35087719	0	0.6	8.065	13809.71751	9485.267	0.664970745
4.1275	35.70175439	4.31E-05	0.7	7.003	11991.22436	8217.4514	0.574917324
4.7625	58.42105263	0.00189692	0.8	6	10273.7586	7020.07	0.48986687
			0.9	5.226	8948.416137	6096.0688	0.424234716
			1	4.535	7765.196959	5271.153	0.365640634
			1.1	4.013	6871.361342	4647.9894	0.321377088
			1.2	3.59	6147.046274	4143.012	0.285508352
			1.3	4.47	7653.895589	5193.556	0.36012889
			1.4	2.977	5097.38874	3411.2126	0.233528364
			1.5	2.568	4397.046274	2922.9484	0.198846774
			1.6	1.946	3331.977781	2180.4048	0.146103621
			1.7	1.406	2407.320247	1535.7528	0.100313745
			1.8	1.032	1766.909288	1089.2716	0.068600017
			1.9	0.771	1319.991479	777.6898	0.046468244
			2	0.688	1177.868192	678.6044	0.03943017
			2.1	0.482	825.1284658	432.6816	0.021962181
			2.2	0.27	462.1147671	179.596	0.003985415
			2.3	0.233	398.7586027	135.4254	0.000847961
			2.4	0.235	402.1832603	137.813	0.001017553
			2.5	0.229	391.9092877	130.6502	0.000508776
			2.6	0.228	390.1969589	129.4564	0.00042398
			2.7	0.223	381.6353151	123.4874	0
			2.8	0.226	386.7723014	127.0688	0.000254388
			2.9	0.227	388.4846301	128.2626	0.000339184
			3	0.227	388.4846301	128.2626	0.000339184
			3.1	0.223	381.6353151	123.4874	0
			3.2	0.225	385.0599726	125.875	0.000169592
			3.3	0.224	383.3476438	124.6812	8.48E-05

Table 13 Data corresponding to the normalized WDS intensities used for the depth profile fit curve for sample E-15

Fit							
Depth (cm)	Normalized Intensity (AU)	Depth (cm)	Normalized Intensity (AU)	Depth (cm)	Normalized Intensity (AU)	Depth (cm)	Normalized Intensity (AU)
0.3	0.978733868	1.008542714	0.388698339	1.762311558	0.091507356	2.516080402	0.012943405
0.315075377	0.963592768	1.02361809	0.379449804	1.777386935	0.088440386	2.531155779	0.012383711
0.330150754	0.948527082	1.038693467	0.37035009	1.792462312	0.0854586	2.546231156	0.011846024
0.345226131	0.933540017	1.053768844	0.361398941	1.807537688	0.082560325	2.561306533	0.011329602
0.360301508	0.918634724	1.068844221	0.352596034	1.822613065	0.079743895	2.57638191	0.010833723
0.375376884	0.903814298	1.083919598	0.343940983	1.837688442	0.077007652	2.591457286	0.010357682
0.390452261	0.889081775	1.098994975	0.335433337	1.852763819	0.074349949	2.606532663	0.009900796
0.405527638	0.874440133	1.114070352	0.327072584	1.867839196	0.071769148	2.62160804	0.009462399
0.420603015	0.859892288	1.129145729	0.318858149	1.882914573	0.069263622	2.636683417	0.009041843
0.435678392	0.845441091	1.144221106	0.3107894	1.89798995	0.066831757	2.651758794	0.008638497
0.450753769	0.831089329	1.159296482	0.302865647	1.913065327	0.064471951	2.666834171	0.008251751
0.465829146	0.816839724	1.174371859	0.295086143	1.928140704	0.062182616	2.681909548	0.00788101
0.480904523	0.802694927	1.189447236	0.287450086	1.94321608	0.059962177	2.696984925	0.007525696
0.495979899	0.788657523	1.204522613	0.279956622	1.958291457	0.057809077	2.712060302	0.007185248
0.511055276	0.774730023	1.21959799	0.272604845	1.973366834	0.055721771	2.727135678	0.006859123
0.526130653	0.760914868	1.234673367	0.265393799	1.988442211	0.053698733	2.742211055	0.006546793
0.54120603	0.747214426	1.249748744	0.258322479	2.003517588	0.051738452	2.757286432	0.006247745
0.556281407	0.733630989	1.264824121	0.251389835	2.018592965	0.049839435	2.772361809	0.005961483
0.571356784	0.720166775	1.279899497	0.244594771	2.033668342	0.048000206	2.787437186	0.005687527
0.586432161	0.706823927	1.294974874	0.237936146	2.048743719	0.04621931	2.802512563	0.005425409
0.601507538	0.693604509	1.310050251	0.231412781	2.063819095	0.044495307	2.81758794	0.005174677
0.616582915	0.680510507	1.325125628	0.225023455	2.078894472	0.04282678	2.832663317	0.004934896
0.631658291	0.66754383	1.340201005	0.218766908	2.093969849	0.041212328	2.847738693	0.00470564
0.646733668	0.654706308	1.355276382	0.212641844	2.109045226	0.039650572	2.86281407	0.004486501
0.661809045	0.64199969	1.370351759	0.206646933	2.124120603	0.038140153	2.877889447	0.004277082
0.676884422	0.629425646	1.385427136	0.200780811	2.13919598	0.036679733	2.892964824	0.004077
0.691959799	0.616985765	1.400502513	0.195042082	2.154271357	0.035267994	2.908040201	0.003885884
0.707035176	0.604681555	1.415577889	0.189429321	2.169346734	0.033903639	2.923115578	0.003703375
0.722110553	0.592514444	1.430653266	0.183941073	2.184422111	0.032585393	2.938190955	0.003529129
0.73718593	0.580485778	1.445728643	0.17857586	2.199497487	0.031312001	2.953266332	0.00336281
0.752261307	0.568596824	1.46080402	0.173332175	2.214572864	0.030082232	2.968341709	0.003204096
0.767336683	0.556848765	1.475879397	0.16820849	2.229648241	0.028894874	2.983417085	0.003052676
0.78241206	0.545242704	1.490954774	0.163203256	2.244723618	0.027748739	2.998492462	0.002908248
0.797487437	0.533779665	1.506030151	0.1583149	2.259798995	0.02664266	3.013567839	0.002770522
0.812562814	0.52246059	1.521105528	0.153541836	2.274874372	0.025575492	3.028643216	0.00263922
0.827638191	0.51128634	1.536180905	0.148882456	2.289949749	0.024546113	3.043718593	0.002514071
0.842713568	0.500257698	1.551256281	0.14433514	2.305025126	0.02355342	3.05879397	0.002394816
0.857788945	0.489375366	1.566331658	0.139898253	2.320100503	0.022596336	3.073869347	0.002281203
0.872864322	0.478639969	1.581407035	0.135570146	2.335175879	0.021673804	3.088944724	0.002172993
0.887939698	0.468052052	1.596482412	0.131349163	2.350251256	0.020784788	3.104020101	0.002069952
0.903015075	0.457612085	1.611557789	0.127233634	2.365326633	0.019928275	3.119095477	0.001971857
0.918090452	0.447320458	1.626633166	0.123221884	2.38040201	0.019103276	3.134170854	0.001878493
0.933165829	0.437177488	1.641708543	0.119312229	2.395477387	0.018308818	3.149246231	0.001789654
0.948241206	0.427183415	1.65678392	0.115502982	2.410552764	0.017543956	3.164321608	0.001705139
0.963316583	0.417338407	1.671859296	0.111792451	2.425628141	0.016807762	3.179396985	0.001624758
0.97839196	0.407642555	1.686934673	0.108178941	2.440703518	0.016099331	3.194472362	0.001548327
0.993467337	0.398095883	1.70201005	0.104660756	2.455778894	0.015417779	3.209547739	0.001475669
		1.717085427	0.101236199	2.470854271	0.014762242	3.224623116	0.001406614
		1.732160804	0.097903575	2.485929648	0.014131879	3.239698492	0.001341
		1.747236181	0.094661191	2.501005025	0.013525867	3.254773869	0.001278669
						3.269849246	0.001219472
						3.284924623	0.001163264
						3.3	0.001109908

Table 14 Raw and normalized data corresponding to the wet chemistry analysis and the WDS analysis of sample I-15 for concentration depth profile

I-15 Depth Profile - WDS						
Wet Chemistry			WDS			
Depth (cm)	Raw ppm	Normalized Intensity (AU)	Depth (cm)	Raw Counts	[Cl] (ppm) CFS Cal	Normalized Intensity (AU)
0.3175	9765.9649	1	0.1	8.664	14835.40244	
0.9525	3760.7895	0.38318557	0.2	9.118	15612.7997	
1.5875	355.52632	0.033418027	0.3	8.386	14359.37504	1
2.2225	31.491228	0.00013515	0.4	7.722	13222.38874	0.918327183
2.8575	32.807018	2.70E-04	0.5	6.761	11576.84079	0.800123001
3.4925	33.508772	0.000342379	0.6	5.888	10081.97778	0.692742927
4.1275	30.175439	0.00E+00	0.7	5.397	9241.224356	0.632349323
4.7625	33.157895	0.000306339	0.8	4.773	8172.731205	0.555596556
			0.9	4.056	6944.991479	0.467404674
			1	3.018	5167.594219	0.339729397
			1.1	2.636	4513.48463	0.292742927
			1.2	1.967	3367.936685	0.210455105
			1.3	1.332	2280.607918	0.132349323
			1.4	0.959	1641.909288	0.086469865
			1.5	0.544	931.2928493	0.035424354
			1.6	0.348	595.676411	0.011316113
			1.7	0.284	486.0873699	0.003444034
			1.8	0.271	463.8270959	0.001845018
			1.9	0.27	462.1147671	0.001722017
			2	0.26	444.9914795	0.000492005
			2.1	0.259	443.2791507	0.000369004
			2.2	0.261	446.7038082	0.000615006
			2.3	0.268	458.6901096	0.001476015
			2.4	0.267	456.9777808	0.001353014
			2.5	0.263	450.1284658	0.000861009
			2.6	0.263	450.1284658	0.000861009
			2.7	0.256	438.1421644	0
			2.8	0.256	438.1421644	0
			2.9	0.267	456.9777808	0.001353014
			3	0.266	455.2654521	0.001230012
			3.1	0.258	441.5668219	0.000246002
			3.2	0.264	451.8407945	0.00098401
			3.3	0.262	448.416137	0.000738007

Table 15 Data corresponding to the normalized WDS intensities used for the depth profile fit curve for sample I-15

Fit							
Depth (cm)	Normalized Intensity (AU)	Depth (cm)	Normalized Intensity (AU)	Depth (cm)	Normalized Intensity (AU)	Depth (cm)	Normalized Intensity (AU)
0.3	1.058208231	1.008542714	0.324144067	1.762311558	0.047520968	2.516080402	0.00407034
0.31507538	1.037955666	1.02361809	0.314071443	1.777386935	0.045412678	2.531155779	0.003881028
0.33015075	1.017845882	1.038693467	0.3042277	1.792462312	0.043386875	2.546231156	0.003702175
0.34522613	0.99788463	1.053768844	0.294610893	1.807537688	0.041440991	2.561306533	0.003533262
0.36030151	0.97807752	1.068844221	0.285218971	1.822613065	0.039572505	2.57638191	0.003373789
0.37537688	0.958430014	1.083919598	0.276049778	1.837688442	0.037778947	2.591457286	0.003223281
0.39045226	0.938947422	1.098994975	0.267101064	1.852763819	0.036057893	2.606532663	0.003081281
0.40552764	0.919634897	1.114070352	0.258370481	1.867839196	0.034406972	2.62160804	0.002947353
0.42060302	0.900497436	1.129145729	0.249855597	1.882914573	0.032823863	2.636683417	0.002821082
0.43567839	0.88153987	1.144221106	0.241553892	1.89798995	0.031306293	2.651758794	0.00270207
0.45075377	0.862766864	1.159296482	0.233462769	1.913065327	0.029852042	2.666834171	0.002589938
0.46582915	0.844182912	1.174371859	0.225579555	1.928140704	0.028458939	2.681909548	0.002484323
0.48090452	0.825792338	1.189447236	0.217901508	1.94321608	0.027124866	2.696984925	0.002384881
0.4959799	0.80759929	1.204522613	0.210425819	1.958291457	0.025847752	2.712060302	0.002291283
0.51105528	0.789607736	1.21959799	0.203149618	1.973366834	0.02462558	2.727135678	0.002203214
0.52613065	0.771821468	1.234673367	0.196069979	1.988442211	0.023456383	2.742211055	0.002120377
0.54120603	0.754244095	1.249748744	0.189183923	2.003517588	0.022338242	2.757286432	0.002042487
0.55628141	0.736879041	1.264824121	0.182488424	2.018592965	0.021269291	2.772361809	0.001969273
0.57135678	0.71972955	1.279899497	0.175980412	2.033668342	0.02024771	2.787437186	0.001900478
0.58643216	0.702798677	1.294974874	0.169656779	2.048743719	0.019271731	2.802512563	0.001835856
0.60150754	0.686089292	1.310050251	0.163514379	2.063819095	0.018339635	2.81758794	0.001775177
0.61658291	0.669604081	1.325125628	0.157550039	2.078894472	0.017449749	2.832663317	0.001718217
0.63165829	0.65334554	1.340201005	0.151760557	2.093969849	0.016600449	2.847738693	0.001664767
0.64673367	0.637315979	1.355276382	0.146142708	2.109045226	0.015790159	2.86281407	0.001614629
0.66180905	0.621517523	1.370351759	0.14069325	2.124120603	0.015017349	2.877889447	0.001567612
0.67688442	0.605952109	1.385427136	0.135408924	2.13919598	0.014280534	2.892964824	0.001523538
0.6919598	0.590621491	1.400502513	0.130286461	2.154271357	0.013578276	2.908040201	0.001482235
0.70703518	0.575527238	1.415577889	0.125322583	2.169346734	0.01290918	2.923115578	0.001443543
0.72211055	0.560670734	1.430653266	0.120514009	2.184422111	0.012271896	2.938190955	0.00140731
0.73718593	0.546053185	1.445728643	0.115857456	2.199497487	0.011665117	2.953266332	0.00137339
0.75226131	0.531675615	1.46080402	0.111349644	2.214572864	0.011087579	2.968341709	0.001341646
0.76733668	0.517538871	1.475879397	0.1069873	2.229648241	0.010538058	2.983417085	0.001311949
0.78241206	0.503643622	1.490954774	0.102767158	2.244723618	0.010015373	2.998492462	0.001284177
0.79748744	0.489990367	1.506030151	0.098685964	2.259798995	0.00951838	3.013567839	0.001258213
0.81256281	0.476579432	1.521105528	0.094740479	2.274874372	0.009045978	3.028643216	0.001233948
0.82763819	0.463410974	1.536180905	0.090927482	2.289949749	0.0085971	3.043718593	0.001211278
0.84271357	0.450484985	1.551256281	0.08724377	2.305025126	0.008170721	3.05879397	0.001190106
0.85778894	0.437801296	1.566331658	0.083686166	2.320100503	0.00776585	3.073869347	0.001170339
0.87286432	0.425359576	1.581407035	0.080251513	2.335175879	0.007381531	3.088944724	0.00115189
0.8879397	0.413159341	1.596482412	0.076936687	2.350251256	0.007016846	3.104020101	0.001134678
0.90301508	0.401199953	1.611557789	0.073738588	2.365326633	0.006670907	3.119095477	0.001118625
0.91809045	0.389480624	1.626633166	0.070654151	2.38040201	0.006342863	3.134170854	0.001103657
0.93316583	0.378000424	1.641708543	0.067680343	2.395477387	0.006031893	3.149246231	0.001089707
0.94824121	0.366758278	1.65678392	0.064814167	2.410552764	0.005737208	3.164321608	0.001076709
0.96331658	0.355752977	1.671859296	0.062052662	2.425628141	0.00545805	3.179396985	0.001064602
0.97839196	0.344983177	1.686934673	0.059392905	2.440703518	0.005193691	3.194472362	0.00105333
0.99346734	0.334447406	1.70201005	0.056832016	2.455778894	0.00494343	3.209547739	0.001042838
		1.717085427	0.054367153	2.470854271	0.004706596	3.224623116	0.001033076
		1.732160804	0.05199552	2.485929648	0.004482544	3.239698492	0.001023995
		1.747236181	0.049714361	2.501005025	0.004270656	3.254773869	0.001015552
						3.269849246	0.001007704
						3.284924623	0.001000411
						3.3	0.000993637

Table 16 Raw and normalized data corresponding to the wet chemistry analysis and the EDS analysis of sample B-15 for concentration depth profile

B-15 Depth Profile - EDS					
Wet Chemistry			EDS		
Depth (cm)	Raw ppm	Normalized Intensity (AU)	Depth (cm)	Raw Counts	Normalized Intensity (AU)
0.3175	9561.7544	1	0.1	4.538	
0.9525	6639.6491	0.69314382	0.2	5.724	
1.5875	3017.6316	0.312788438	0.3	6.397	0.830706781
2.2225	792.63158	0.079136691	0.4	7.041	0.984479465
2.8575	68.947368	3.14E-03	0.5	7.106	1
3.4925	39.035088	0	0.6	6.985	0.971107927
4.1275	41.052632	2.12E-04	0.7	7.07	0.991404011
4.7625	40.438596	0.000147385	0.8	6.462	0.846227316
			0.9	6.174	0.777459408
			1	5.806	0.689589303
			1.1	5.542	0.626552053
			1.2	5.447	0.603868195
			1.3	4.938	0.482330468
			1.4	4.921	0.478271251
			1.5	4.45	0.365807068
			1.6	4.32	0.334765998
			1.7	4.141	0.292024833
			1.8	3.736	0.195319962
			1.9	3.677	0.181232092
			2	3.49	0.136580707
			2.1	3.468	0.131327603
			2.2	3.305	0.092406877
			2.3	3.173	0.060888252
			2.4	3.068	0.035816619
			2.5	2.918	0
			2.6	2.976	0.013849093
			2.7	3.036	0.02817574

Table 17 Data corresponding to the normalized EDS intensities used for the depth profile fit curve for sample B-15

Fit							
Depth (cm)	Normalized Intensity (AU)	Depth (cm)	Normalized Intensity (AU)	Depth (cm)	Normalized Intensity (AU)	Depth (cm)	Normalized Intensity (AU)
0.3	1.125076936	0.86683417	0.714679669	1.4698492	0.386683898	2.07286432	0.18643253
0.3120603	1.115655932	0.87889447	0.706882757	1.4819095	0.381462898	2.08492462	0.183587068
0.3241206	1.106254985	0.89095477	0.699132509	1.4939698	0.376294474	2.09698492	0.180781837
0.3361809	1.096874827	0.90301508	0.691429278	1.5060302	0.371178518	2.10904523	0.178016496
0.3482412	1.087516181	0.91507538	0.68377341	1.5180905	0.366114915	2.12110553	0.175290704
0.3603015	1.078179768	0.92713568	0.67616524	1.5301508	0.361103541	2.13316583	0.172604114
0.3723618	1.068866301	0.93919598	0.668605095	1.5422111	0.356144268	2.14522613	0.169956382
0.3844221	1.05957649	0.95125628	0.661093289	1.5542714	0.351236956	2.15728643	0.167347161
0.3964824	1.050311038	0.96331658	0.653630129	1.5663317	0.346381462	2.16934673	0.164776102
0.4085427	1.041070642	0.97537688	0.646215911	1.578392	0.341577635	2.18140704	0.162242856
0.420603	1.031855993	0.98743719	0.638850919	1.5904523	0.336825315	2.19346734	0.159747072
0.4326633	1.022667777	0.99949749	0.631535429	1.6025126	0.332124338	2.20552764	0.157288398
0.4447236	1.013506672	1.01155779	0.624269709	1.6145729	0.327474533	2.21758794	0.154866484
0.4567839	1.004373351	1.02361809	0.617054012	1.6266332	0.32287572	2.22964824	0.152480974
0.4688442	0.995268479	1.03567839	0.609888586	1.6386935	0.318327716	2.24170854	0.150131516
0.4809045	0.986192715	1.04773869	0.602773665	1.6507538	0.313830329	2.25376884	0.147817756
0.4929648	0.977146712	1.05979899	0.595709477	1.6628141	0.309383363	2.26582915	0.145539338
0.5050251	0.968131114	1.0718593	0.588696236	1.6748744	0.304986614	2.27788945	0.143295908
0.5170854	0.95914656	1.0839196	0.581734149	1.6869347	0.300639874	2.28994975	0.141087111
0.5291457	0.95019368	1.0959799	0.574823412	1.698995	0.296342927	2.30201005	0.13891259
0.541206	0.941273097	1.1080402	0.567964211	1.7110553	0.292095553	2.31407035	0.13677199
0.5532663	0.932385427	1.1201005	0.561156723	1.7231156	0.287897527	2.32613065	0.134664956
0.5653266	0.923531277	1.1321608	0.554401114	1.7351759	0.283748615	2.33819095	0.132591133
0.5773869	0.914711248	1.14422111	0.547697542	1.7472362	0.279648582	2.35025126	0.130550164
0.5894472	0.905925932	1.15628141	0.541046153	1.7592965	0.275597185	2.36231156	0.128541695
0.6015075	0.897175913	1.16834171	0.534447084	1.7713568	0.271594178	2.37437186	0.126565371
0.6135678	0.888461768	1.18040201	0.527900464	1.7834171	0.267639307	2.38643216	0.124620837
0.6256281	0.879784063	1.19246231	0.52140641	1.7954774	0.263732316	2.39849246	0.122707741
0.6376884	0.871143358	1.20452261	0.514965031	1.8075377	0.259872944	2.41055276	0.120825728
0.6497487	0.862540204	1.21658291	0.508576425	1.819598	0.256060923	2.42261307	0.118974447
0.661809	0.853975144	1.22864322	0.502240684	1.8316583	0.252295983	2.43467337	0.117153545
0.6738693	0.845448711	1.24070352	0.495957886	1.8437186	0.248577849	2.44673367	0.115362671
0.6859296	0.83696143	1.25276382	0.489728102	1.8557789	0.244906241	2.45879397	0.113601476
0.6979899	0.828513818	1.26482412	0.483551393	1.8678392	0.241280876	2.47085427	0.111869609
0.7100503	0.82010638	1.27688442	0.477427813	1.8798995	0.237701467	2.48291457	0.110166724
0.7221106	0.811739616	1.28894472	0.471357404	1.8919598	0.234167721	2.49497487	0.108492473
0.7341709	0.803414014	1.30100503	0.4653402	1.9040201	0.230679343	2.50703518	0.106846509
0.7462312	0.795130055	1.31306533	0.459376226	1.9160804	0.227236036	2.51909548	0.105228489
0.7582915	0.786888209	1.32512563	0.453465498	1.9281407	0.223837495	2.53115578	0.103638069
0.7703518	0.778688937	1.33718593	0.447608022	1.940201	0.220483416	2.54321608	0.102074907
0.7824121	0.770532691	1.34924623	0.441803799	1.9522613	0.21717349	2.55527638	0.100538662
0.7944724	0.762419913	1.36130653	0.436052816	1.9643216	0.213907405	2.56733668	0.099028995
0.8065327	0.754351038	1.37336683	0.430355055	1.9763819	0.210684844	2.57939698	0.097545569
0.818593	0.746326487	1.38542714	0.424710489	1.9884422	0.207505491	2.59145729	0.096088048
0.8306533	0.738346676	1.39748744	0.419119081	2.0005025	0.204369023	2.60351759	0.094656096
0.8427136	0.730412008	1.40954774	0.413580787	2.0125628	0.201275118	2.61557789	0.093249382
0.8547739	0.722522877	1.42160804	0.408095555	2.0246231	0.19822345	2.62763819	0.091867574
		1.43366834	0.402663323	2.0366834	0.195213689	2.63969849	0.090510343
		1.44572864	0.397284022	2.0487437	0.192245504	2.65175879	0.089177362
		1.45778894	0.391957575	2.060804	0.189318563	2.6638191	0.087868306
						2.6758794	0.08658285
						2.6879397	0.085320674
						2.7	0.084081458

Table 18 Raw and normalized data corresponding to the wet chemistry analysis and the EDS analysis of sample E-15 for concentration depth profile

E-15 Depth Profile - EDS					
Wet Chemistry			EDS		
Depth (cm)	Raw ppm	Normalized Intensity (AU)	Depth (cm)	Raw Counts	Normalized Intensity (AU)
0.3175	12243.50877	1	0.1	3.662	
0.9525	5224.736842	0.425082451	0.2	4.089	
1.5875	1774.824561	0.142484534	0.3	4.049	1
2.2225	92.36842105	0.004677631	0.4	3.759	0.873029772
2.8575	35.61403509	2.16E-05	0.5	3.566	0.788528897
3.4925	35.35087719	0	0.6	3.239	0.645359019
4.1275	35.70175439	4.31E-05	0.7	3.077	0.574430823
4.7625	58.42105263	0.00189692	0.8	2.843	0.471978984
			0.9	2.774	0.441768827
			1	2.652	0.388353765
			1.1	2.543	0.340630473
			1.2	2.635	0.380910683
			1.3	2.36	0.260507881
			1.4	2.382	0.270140105
			1.5	2.295	0.232049037
			1.6	2.209	0.194395797
			1.7	2.097	0.145359019
			1.8	1.924	0.069614711
			1.9	1.958	0.084500876
			2	1.8	0.015323993
			2.1	1.813	0.021015762
			2.2	1.805	0.017513135
			2.3	1.787	0.009632224
			2.4	1.817	0.022767075
			2.5	1.765	0
			2.6	1.819	0.023642732
			2.7	1.861	0.042031524

Table 19 Data corresponding to the normalized EDS intensities used for the depth profile fit curve for sample E-15

Fit							
Depth (cm)	Normalized Intensity (AU)	Depth (cm)	Normalized Intensity (AU)	Depth (cm)	Normalized Intensity (AU)	Depth (cm)	Normalized Intensity (AU)
0.3	0.957180641	0.86683417	0.488221755	1.469849246	0.188422826	2.072864322	0.06398202
0.312060302	0.94575959	0.87889447	0.480106996	1.481909548	0.184490246	2.084924623	0.062668186
0.324120603	0.934382423	0.89095477	0.472079747	1.493969849	0.180628906	2.096984925	0.061387715
0.336180905	0.923050657	0.90301508	0.464140246	1.506030151	0.176838082	2.109045226	0.060139944
0.348241206	0.911765791	0.91507538	0.456288701	1.518090452	0.173117038	2.121105528	0.05892422
0.360301508	0.900529302	0.92713568	0.448525293	1.530150754	0.169465033	2.133165829	0.057739895
0.372361809	0.889342647	0.93919598	0.440850174	1.542211055	0.165881321	2.145226131	0.056586331
0.384422111	0.878207262	0.95125628	0.433263471	1.554271357	0.162365146	2.157286432	0.055462895
0.396482412	0.867124561	0.96331658	0.425765279	1.566331658	0.15891575	2.169346734	0.054368963
0.408542714	0.856095936	0.97537688	0.418355668	1.57839196	0.155532367	2.181407035	0.053303919
0.420603015	0.845122756	0.98743719	0.411034683	1.590452261	0.152214228	2.193467337	0.052267155
0.432663317	0.834206367	0.99949749	0.403802337	1.602512563	0.14896056	2.205527638	0.051258069
0.444723618	0.823348089	1.01155779	0.396658622	1.614572864	0.145770583	2.21758794	0.050276069
0.45678392	0.812549221	1.02361809	0.389603501	1.626633166	0.142643517	2.229648241	0.04932057
0.468844221	0.801811036	1.03567839	0.382636911	1.638693467	0.139578577	2.241708543	0.048390995
0.480904523	0.79113478	1.04773869	0.375758766	1.650753769	0.136574975	2.253768844	0.047486775
0.492964824	0.780521676	1.05979899	0.368968953	1.66281407	0.133631922	2.265829146	0.04660735
0.505025126	0.76997292	1.0718593	0.362267334	1.674874372	0.130748626	2.277889447	0.045752167
0.517085427	0.759489681	1.0839196	0.355653748	1.686934673	0.127924295	2.289949749	0.044920681
0.529145729	0.749073103	1.0959799	0.349128009	1.698994975	0.125158133	2.30201005	0.044112356
0.54120603	0.738724302	1.1080402	0.342689909	1.711055276	0.122449347	2.314070352	0.043326663
0.553266332	0.728444366	1.1201005	0.336339216	1.723115578	0.11979714	2.326130653	0.042563084
0.565326633	0.718234356	1.1321608	0.330075674	1.735175879	0.117200717	2.338190955	0.041821105
0.577386935	0.708095305	1.14422111	0.323899008	1.747236181	0.114659283	2.350251256	0.041100223
0.589447236	0.698028218	1.15628141	0.317808918	1.759296482	0.112172043	2.362311558	0.040399942
0.601507538	0.688034071	1.16834171	0.311805084	1.771356784	0.109738204	2.374371859	0.039719775
0.613567839	0.678113812	1.18040201	0.305887164	1.783417085	0.107356974	2.386432161	0.039059242
0.625628141	0.668268359	1.19246231	0.300054798	1.795477387	0.105027562	2.398492462	0.038417873
0.637688442	0.658498602	1.20452261	0.294307604	1.807537688	0.102749179	2.410552764	0.037795202
0.649748744	0.648805402	1.21658291	0.28864518	1.81959799	0.100521039	2.422613065	0.037190777
0.661809045	0.639189588	1.22864322	0.283067105	1.831658291	0.098342359	2.434673367	0.036604148
0.673869347	0.629651964	1.24070352	0.277572942	1.843718593	0.096212358	2.446733668	0.036034877
0.685929648	0.620193299	1.25276382	0.272162233	1.855778894	0.094130256	2.45879397	0.035482533
0.69798995	0.610814336	1.26482412	0.266834503	1.867839196	0.092095281	2.470854271	0.034946691
0.710050251	0.601515788	1.27688442	0.261589259	1.879899497	0.090106662	2.482914573	0.034426936
0.722110553	0.592298335	1.28894472	0.256425993	1.891959799	0.088163631	2.494974874	0.033922861
0.734170854	0.583162631	1.30100503	0.251344181	1.904020101	0.086265426	2.507035176	0.033434064
0.746231156	0.574109296	1.31306533	0.24634328	1.916080402	0.084411288	2.519095477	0.032960154
0.758291457	0.565138924	1.32512563	0.241422735	1.928140704	0.082600465	2.531155779	0.032500745
0.770351759	0.556252076	1.33718593	0.236581975	1.940201005	0.080832207	2.54321608	0.032055459
0.78241206	0.547449285	1.34924623	0.231820415	1.952261307	0.07910577	2.555276382	0.031623928
0.794472362	0.538731052	1.36130653	0.227137456	1.964321608	0.077420417	2.567336683	0.031205787
0.806532663	0.53009785	1.37336683	0.222532485	1.97638191	0.075775415	2.579396985	0.030800683
0.818592965	0.521550121	1.38542714	0.218004877	1.988442211	0.074170035	2.591457286	0.030408266
0.830653266	0.513088279	1.39748744	0.213553996	2.000502513	0.072603558	2.603517588	0.030028197
0.842713568	0.504712706	1.40954774	0.209179191	2.012562814	0.071075267	2.615577889	0.029660141
0.854773869	0.496423756	1.42160804	0.204879803	2.024623116	0.069584453	2.627638191	0.029303771
		1.43366834	0.200655159	2.036683417	0.068130414	2.639698492	0.028958769
		1.44572864	0.196504577	2.048743719	0.066712455	2.651758794	0.02862482
		1.45778894	0.192427367	2.06080402	0.065329884	2.663819095	0.02830162
						2.675879397	0.027988868
						2.687939698	0.027686271
						2.7	0.027393545

Table 20 Raw and normalized data corresponding to the wet chemistry analysis and the EDS analysis of sample I-15 for concentration depth profile

I-15 Depth Profile - EDS					
Wet Chemistry			EDS		
Depth (cm)	Raw ppm	Normalized Intensity (AU)	Depth (cm)	Raw Counts	Normalized Intensity (AU)
0.3175	9765.9649	1	0.1	5.016	
0.9525	3760.7895	0.38318557	0.2	5.53	
1.5875	355.52632	0.033418027	0.3	5.27	1
2.2225	31.491228	0.00013515	0.4	5.084	0.92700157
2.8575	32.807018	2.70E-04	0.5	4.988	0.889324961
3.4925	33.508772	0.000342379	0.6	4.455	0.680141287
4.1275	30.175439	0.00E+00	0.7	4.422	0.667189953
4.7625	33.157895	0.000306339	0.8	4.024	0.510989011
			0.9	3.996	0.5
			1	3.779	0.414835165
			1.1	3.517	0.312009419
			1.2	3.504	0.306907378
			1.3	3.24	0.203296703
			1.4	3.212	0.192307692
			1.5	3.011	0.113422292
			1.6	2.848	0.049450549
			1.7	2.827	0.041208791
			1.8	2.722	0
			1.9	2.816	0.03689168
			2	2.738	0.006279435
			2.1	2.793	0.027864992
			2.2	2.75	0.010989011
			2.3	2.791	0.027080063
			2.4	2.804	0.032182104
			2.5	2.735	0.005102041
			2.6	2.749	0.010596546
			2.7	2.922	0.078492936

Table 21 Data corresponding to the normalized EDS intensities used for the depth profile fit curve for sample I-15

Fit							
Depth (cm)	Normalized Intensity (AU)	Depth (cm)	Normalized Intensity (AU)	Depth (cm)	Normalized Intensity (AU)	Depth (cm)	Normalized Intensity (AU)
0.3	1.061231081	0.8668342	0.472115879	1.46984925	0.152436631	2.07286432	0.052533455
0.3120603	1.046249205	0.8788945	0.462625854	1.48190955	0.148831064	2.08492462	0.051700028
0.3241206	1.031344186	0.8909548	0.453272305	1.49396985	0.145312493	2.09698492	0.050894753
0.3361809	1.016518577	0.9030151	0.444055102	1.50603015	0.1418795	2.10904523	0.050116834
0.3482412	1.001774885	0.9150754	0.434974061	1.51809045	0.138530671	2.12110553	0.04936549
0.3603015	0.987115571	0.9271357	0.42602895	1.53015075	0.13526459	2.13316583	0.048639959
0.3723618	0.972543051	0.939196	0.417219486	1.54221106	0.132079846	2.14522613	0.047939492
0.3844221	0.958059689	0.9512563	0.408545335	1.55427136	0.128975032	2.15728643	0.047263359
0.3964824	0.9436678	0.9633166	0.400006118	1.56633166	0.125948741	2.16934673	0.046610843
0.4085427	0.92936965	0.9753769	0.391601404	1.57839196	0.122999576	2.18140704	0.045981245
0.420603	0.91516745	0.9874372	0.383330721	1.59045226	0.120126141	2.19346734	0.045373881
0.4326633	0.901063361	0.9994975	0.375193548	1.60251256	0.117327048	2.20552764	0.044788081
0.4447236	0.887059489	1.0115578	0.367189322	1.61457286	0.114600916	2.21758794	0.044223193
0.4567839	0.873157885	1.0236181	0.359317434	1.62663317	0.111946371	2.22964824	0.043678578
0.4688442	0.859360546	1.0356784	0.351577237	1.63869347	0.109362046	2.24170854	0.043153613
0.4809045	0.84566941	1.0477387	0.343968038	1.65075377	0.106846584	2.25376884	0.04264769
0.4929648	0.832086361	1.059799	0.336489108	1.66281407	0.104398637	2.26582915	0.042160215
0.5050251	0.818613223	1.0718593	0.329139678	1.67487437	0.102016866	2.27788945	0.041690608
0.5170854	0.805251763	1.0839196	0.321918941	1.68693467	0.099699943	2.28994975	0.041238305
0.5291457	0.79200369	1.0959799	0.314826053	1.69899497	0.09744655	2.30201005	0.040802754
0.541206	0.778870651	1.1080402	0.307860135	1.71105528	0.09525538	2.31407035	0.040383419
0.5532663	0.765854236	1.1201005	0.301020274	1.72311558	0.09312514	2.32613065	0.039979775
0.5653266	0.752955972	1.1321608	0.294305525	1.73517588	0.091054546	2.33819095	0.039591313
0.5773869	0.740177328	1.1442211	0.287714907	1.74723618	0.089042328	2.35025126	0.039217537
0.5894472	0.727519711	1.1562814	0.281247413	1.75929648	0.08708723	2.36231156	0.038857962
0.6015075	0.714984465	1.1683417	0.274902004	1.77135678	0.085188006	2.37437186	0.038512118
0.6135678	0.702572876	1.180402	0.268677612	1.78341709	0.083343428	2.38643216	0.038179546
0.6256281	0.690286165	1.1924623	0.262573143	1.79547739	0.081552279	2.39849246	0.037859801
0.6376884	0.678125494	1.2045226	0.256587477	1.80753769	0.079813356	2.41055276	0.037552449
0.6497487	0.666091963	1.2165829	0.250719467	1.81959799	0.078125473	2.42261307	0.037257069
0.661809	0.654186607	1.2286432	0.244967944	1.83165829	0.076487458	2.43467337	0.03697325
0.6738693	0.642410404	1.2407035	0.239331717	1.84371859	0.074898152	2.44673367	0.036700595
0.6859296	0.630764268	1.2527638	0.233809572	1.85577889	0.073356414	2.45879397	0.036438715
0.6979899	0.61924905	1.2648241	0.228400275	1.8678392	0.071861118	2.47085427	0.036187236
0.7100503	0.607865542	1.2768844	0.223102573	1.8798995	0.070411152	2.48291457	0.035945792
0.7221106	0.596614474	1.2889447	0.217915195	1.8919598	0.069005422	2.49497487	0.035714029
0.7341709	0.585496515	1.301005	0.212836854	1.9040201	0.067642849	2.50703518	0.035491603
0.7462312	0.574512275	1.3130653	0.207866244	1.9160804	0.066322371	2.51909548	0.035278181
0.7582915	0.563662302	1.3251256	0.203002049	1.9281407	0.065042942	2.53115578	0.035073437
0.7703518	0.552947084	1.3371859	0.198242935	1.94020101	0.063803531	2.54321608	0.03487706
0.7824121	0.542367051	1.3492462	0.193587559	1.95226131	0.062603127	2.55527638	0.034688743
0.7944724	0.531922574	1.3613065	0.189034563	1.96432161	0.061440732	2.56733668	0.034508193
0.8065327	0.521613966	1.3733668	0.184582582	1.97638191	0.060315366	2.57939698	0.034335123
0.818593	0.511441481	1.3854271	0.180230239	1.98844221	0.059226067	2.59145729	0.034169256
0.8306533	0.501405316	1.3974874	0.175976151	2.00050251	0.058171888	2.60351759	0.034010324
0.8427136	0.491505613	1.4095477	0.171818925	2.01256281	0.057151899	2.61557789	0.033858068
0.8547739	0.481742457	1.421608	0.167757163	2.02462312	0.056165189	2.62763819	0.033712236
		1.4336683	0.163789462	2.03668342	0.05521086	2.63969849	0.033572585
		1.4457286	0.159914415	2.04874372	0.054288034	2.65175879	0.033438879
		1.4577889	0.156130609	2.06080402	0.053395848	2.6638191	0.033310891
						2.6758794	0.0331884
						2.6879397	0.033071194
						2.7	0.032959067

2) <u>FDOT SEM 6400 Mapping Guide</u>

- Load sample
- Ensure that the microscope X-Y stage axes are centered (X: 25 mm, Y:35 mm)
- Turn on Deben Sprite Two Axis Stage Controller using red power switch in the rear of the Deben labeled box on top of the SEM housing

- Bring down the Sprite control module with display and joystick and confirm that the coordinates displayed match with those shown on each axis' mechanical counter
- Bring up SEM system to operating conditions
- Select proper "job" in the Link ISIS software
  - The map data will be saved to the job's directory but only 1000 map group images may be saved per job, so it is wise to open Speedmap (grid icon on X-Ray Analysis window) and use the "Open or Delete a Spectrum" dialog to confirm that sufficient space is available prior to beginning any automated collection, creating a new job if necessary
- Turn on attached picoammeter and set scale properly then set the probe current as desired for consistent collection results, using the far right white button above the five fault lights on the SEM table itself to toggle the Probe Current Detector
  - Note that the filament typically takes 45-60 minutes to stabilize, and may take considerably longer if it has been recently replaced; wait for stability to get the best mapping results
- Open the Isisbin/wxAStg/wxAStg.exe program
  - Click the Edit->Insert Pattern button to generate a rectangular grid with the appropriate stage coordinates
  - Click the File->Start Run button to bring up the run dialog
- Open the ISIS Auto program
  - Click the Edit->Auto Setup button and click the No X-ray Acquisition setting at the top, Beam mode: Scan, Imaging: Acquire X-ray maps
  - Click the record button to generate the total number of points indicated on the wxAStg run dialog
- Return to wxAStg and click the Make Ready button to move the stage to the starting position
- Return to ISIS Auto, click Edit->Select All then click the Play button, select Single Auto Run and click Start

- Within a few seconds return to wxAStg again and click the Start Run button
- The two programs should now be in synchronized operation
- Your automated collection should be underway and the stage should move automatically between the grid points indicated in wxAStg
- When finished, center the stage and turn off the Deben Sprite Stage Controller again using the switch in the back then shutdown the SEM as normal
    - Be sure to switch the ISIS job back to “Job number 1” for the next user
- To batch convert your map data files from proprietary ISIS format into standard tab separated variable (TSV) you may use the Edit->Process Data dialog in wxAStg and select the proper ISIS job directory
    - Note that at the time of writing the wxAStg Generate Montage functionality is incomplete and should not be used, the ImageJ macros are instead provided separately

3) <u>Loading FLEXTRAN Program on TN-5500 System</u>

This procedure usually only needs to be redone if the TN-5500 has been rebooted since the last program load.

- On the TN-5500:
    - Press ESC to exit TASK if necessary so you are at a basic FLEXTRAN prompt
    - If an asterisk appears in the upper left, press CTRL+A (toggle echo) then press ESC again
    - Flip the small black switch in the back to the UP position (terminal input enabled)
- Open Windows Explorer and navigate to the AutoProbe\CLI folder
- Run AutoProbe_CLI.exe
- At the command prompt on the PC:
    - Type *init 3*

        - The number (3 here) is the COM port that is being used, same as in HyperTerminal connection
    - Type *sendfile FT_LScan_Fast.flxt 50 250*
        - You should see the commands being sent on the TN-5500 screen and the PC command prompt will say "Done" when finished
    - Type *quit*

4) <u>Running FDOT samples with AutoProbe</u>

- Load sample into system
- In the menu use **Insert->Rectangle** to specify a new region of interest (ROI) to collect
    - A rectangle will be created with default parameters. To change its position and parameters, click on its name (default: "New Rect") in the **Objects** list on the upper right and input new values in the table that appears in the lower right. Please make sure that X1 < X2 and Y1 < Y2 before you start a collection or odd things might happen
    - You may insert as many ROI objects as desired for the run, but one works fine for all the samples so far
- In the menu, go to **Tools->Calibrate Z**
    - This process will take 3 points and mathematically determine a 3D plane containing them, approximating a perfectly uniform flat surface. The plane will then be used to link any X, Y position to a corresponding Z height
    - Choose any 3 points that appear to be as well polished as possible and enter their X,Y,Z coordinates using the optical microscope to determine Z. The points being spread out across the ROI will give the best results
- **Pre-Execute Checklist**
    - Beam current, spot size, e-beam focus, etc. all set as desired for run

- The TN-5500 is sitting at FLEXTRAN prompt and **echo is off**, that is no asterisk appears when you press ESC
- The small black switch beside the terminal and keyboard connections on the back of the TN-5500 system flipped in the UP position (terminal input enabled)
- Confirm that each object has the proper parameters set

- In the menu click **Run->Execute**